

RESEARCH ARTICLE

# Interferon- $\gamma$ Inhibits Ebola Virus Infection

Bethany A. Rhein<sup>1</sup>, Linda S. Powers<sup>2</sup>, Kai Rogers<sup>1</sup>, Manu Anantpadma<sup>3</sup>, Brajesh K. Singh<sup>4</sup>, Yasuteru Sakurai<sup>3</sup>, Thomas Bair<sup>5</sup>, Catherine Miller-Hunt<sup>1\*</sup>, Patrick Sinn<sup>4</sup>, Robert A. Davey<sup>3</sup>, Martha M. Monick<sup>2</sup>, Wendy Maury<sup>1</sup>✉\*

**1** Department of Microbiology, The University of Iowa, Iowa City, Iowa, United States of America, **2** Department of Internal Medicine, The University of Iowa, Iowa City, Iowa, United States of America, **3** Department of Virology and Immunology, Texas Biomedical Research Institute, San Antonio, Texas, United States of America, **4** Department of Pediatrics, The University of Iowa, Iowa City, Iowa, United States of America, **5** Iowa Institute for Human Genetics, The University of Iowa, Iowa City, Iowa, United States of America

✉ These authors contributed equally to this work.

✉ Current address: Department of Biological Sciences, Western Illinois University, Macomb, Illinois, United States of America

\* [wendy-maury@uiowa.edu](mailto:wendy-maury@uiowa.edu)



CrossMark

click for updates

## OPEN ACCESS

**Citation:** Rhein BA, Powers LS, Rogers K, Anantpadma M, Singh BK, Sakurai Y, et al. (2015) Interferon- $\gamma$  Inhibits Ebola Virus Infection. PLoS Pathog 11(11): e1005263. doi:10.1371/journal.ppat.1005263

**Editor:** Matthias Johannes Schnell, Thomas Jefferson University, UNITED STATES

**Received:** April 19, 2015

**Accepted:** October 19, 2015

**Published:** November 12, 2015

**Copyright:** © 2015 Rhein et al. This is an open access article distributed under the terms of the [Creative Commons Attribution License](https://creativecommons.org/licenses/by/4.0/), which permits unrestricted use, distribution, and reproduction in any medium, provided the original author and source are credited.

**Data Availability Statement:** All gene array files are available from the GEO repository database (accession number, GSE64997).

**Funding:** This research was supported by the following grants from National Institutes of Health: RO1AI077519 to WM and RO1 HL096625 and R21HL109589 to MMM. MMM also received support from the University of Iowa Environmental Health Sciences Research Center that is supported by P30ES005605. CMH was funded by NIH T32AU996343. The Ewing Halsell Foundation (<http://www.ewinghalsell.org/includes/index.php>) provided support to RAD along with the Department of

## Abstract

Ebola virus outbreaks, such as the 2014 Makona epidemic in West Africa, are episodic and deadly. Filovirus antivirals are currently not clinically available. Our findings suggest interferon gamma, an FDA-approved drug, may serve as a novel and effective prophylactic or treatment option. Using mouse-adapted Ebola virus, we found that murine interferon gamma administered 24 hours before or after infection robustly protects lethally-challenged mice and reduces morbidity and serum viral titers. Furthermore, we demonstrated that interferon gamma profoundly inhibits Ebola virus infection of macrophages, an early cellular target of infection. As early as six hours following *in vitro* infection, Ebola virus RNA levels in interferon gamma-treated macrophages were lower than in infected, untreated cells. Addition of the protein synthesis inhibitor, cycloheximide, to interferon gamma-treated macrophages did not further reduce viral RNA levels, suggesting that interferon gamma blocks life cycle events that require protein synthesis such as virus replication. Microarray studies with interferon gamma-treated human macrophages identified more than 160 interferon-stimulated genes. Ectopic expression of a select group of these genes inhibited Ebola virus infection. These studies provide new potential avenues for antiviral targeting as these genes that have not previously appreciated to inhibit negative strand RNA viruses and specifically Ebola virus infection. As treatment of interferon gamma robustly protects mice from lethal Ebola virus infection, we propose that interferon gamma should be further evaluated for its efficacy as a prophylactic and/or therapeutic strategy against filoviruses. Use of this FDA-approved drug could rapidly be deployed during future outbreaks.

## Author Summary

Filovirus outbreaks occur sporadically, but with increasing frequency. With no current approved filovirus therapeutics, the 2014 Makona Ebola virus epidemic in Guinea, Sierra

Defense (HDTRA-1-12-1-00-2). The funders had no role in study design, data collection and analysis, decision to publish, or preparation of the manuscript.

**Competing Interests:** The authors have declared that no competing interests exist.

Leone and Liberia emphasizes the need for effective treatments against this highly pathogenic family of viruses. The use of this FDA-approved drug to inhibit Ebola virus infection would allow rapid implementation of a novel antiviral therapy for future crises. Interferon gamma elicits an antiviral state in antigen-presenting cells and stimulates cellular immune responses. We demonstrate that interferon gamma profoundly inhibits Ebola virus infection of macrophages, which are early cellular targets of Ebola virus. We also identify novel interferon gamma-stimulated genes in human macrophage populations that have not been previously appreciated to inhibit filoviruses or other negative strand RNA viruses. Finally and most importantly, we show that interferon gamma given 24 hours prior to or after virus infection protects mice from lethal Ebola virus challenge, suggesting that this drug may serve as an effective prophylactic and/or therapeutic strategy against this deadly virus.

## Introduction

Ebola virus (EBOV) is a member of the genus *Ebolavirus* within the *Filoviridae* family of highly pathogenic viruses. These viruses cause a severe hemorrhagic fever syndrome in humans and non-human primates (NHP). EBOV infection frequently is associated with high mortality rates and is responsible for the devastating 2014 West African EBOV outbreak [1, 2]. This outbreak has generated a renewed emphasis on the development and approval of safe, effective prophylactics and therapeutics against the virus.

Macrophages and dendritic cells (DCs) play an important role in EBOV pathogenesis as sites of early and sustained virus replication [3, 4]. EBOV infection causes dysregulation of these antigen-presenting cells, increasing production and release of pro-inflammatory proteins, vasoactive molecules, and coagulation factors [5–7]. Pro-inflammatory molecules recruit other target cells to the site of infection, providing additional cells for virus infection and increasing circulation of inflammatory cells and proteins. This uncontrolled amplification of infection and cytokine production results in dysregulation of the inflammatory response, leading to the systemic spread of the virus, excessive cytokine accumulation and circulatory collapse observed in cases of fatal EBOV hemorrhagic fever in humans and non-human primates [3, 4, 6, 8]. Contributing to this amplifying dysregulation, EBOV sustains replication in macrophages and DCs by counteracting early innate immune responses, thereby decreasing effective host responses to the virus [5, 9]. These events in combination with decreased T cell numbers observed in EBOV-infected individuals [10] are thought to lead to poor adaptive immune responses to infection.

Disruption of EBOV infection in macrophages would be predicted to decrease virus loads and associated virus-induced cytokine dysfunction. One approach to controlling virus replication in macrophages is to elicit early innate immune responses. If these responses could be triggered prior to virus-mediated inhibition of these responses, systemic control of EBOV replication should be possible. Previous studies have investigated the ability of type I interferons (IFNs) to decrease EBOV morbidity and mortality with mixed results [11–13]. Jahrling et al. demonstrated that administration of IFN- $\alpha$ 2b by itself did not significantly alter the course of EBOV in cynomolgus macaques, but more recently IFN- $\beta$  was shown to prolong survival in rhesus macaques [11, 12]. Additionally, the combination of type I IFN with three monoclonal antibodies (mAbs) against EBOV glycoprotein (GP) provided robust protection against lethal challenge, while neither the IFN nor mAbs alone was highly efficacious [13].

The ability of IFNs other than type I IFN to control EBOV infection has not been explored and several lines of reasoning suggest that type II IFN, interferon gamma (IFN $\gamma$ ), would inhibit EBOV infection of macrophages. Macrophages treated with IFN $\gamma$  alone or in combination with tumor necrosis factor alpha (TNF $\alpha$ ) are activated towards a M1 phenotype that is characteristically proinflammatory and antiviral, enhancing host defenses [14–16]. As IFN $\gamma$  directly stimulates the expression of a number of interferon-stimulated genes (ISGs) having antiviral activity [17, 18], IFN $\gamma$  treatment would be predicted to generate macrophages that are resistant to EBOV infection. Since it is thought that EBOV infection of macrophages is responsible for dysregulated cytokine production, reducing infection would likely reduce aberrant cytokine production concomitantly. Finally, as IFN $\gamma$  potently activates T cell responses through enhancement of phagocytosis and antigen presentation [19], such stimulation of antigen presentation would be predicted to enhance adaptive immune responses to *in vivo* infection.

Here, we demonstrate that IFN $\gamma$  blocks EBOV infection of murine peritoneal macrophages and robustly protects mice from fatal EBOV infection when administered as late as 24 hours following infection. We also identified novel IFN $\gamma$ -stimulated genes that inhibit EBOV infection, defining new downstream mechanisms through which this FDA-approved drug functions. During these studies, we evaluated IFN $\gamma$  inhibition of a BSL2 model virus of EBOV, recombinant vesicular stomatitis virus (VSV) encoding EBOV glycoprotein (EBOV GP/rVSV), in interferon  $\alpha/\beta$  receptor knock out (IFNAR<sup>-/-</sup>) mice. IFN $\gamma$  was highly effective at inhibiting infection by this recombinant virus. Comparative use of this recombinant BSL2 virus in parallel with EBOV and wild-type VSV permitted us to evaluate the mechanism of IFN $\gamma$  inhibition in greater detail. These latter findings suggest that IFN $\gamma$  may have efficacy not only against EBOV, but also a broader range of *Mononegavirales*.

## Results

### IFN $\gamma$ blocks EBOV and EBOV GP/rVSV infection of primary macrophages

Mouse peritoneal macrophages treated for 48 hours with either granulocyte-macrophage colony stimulating factor (GM-CSF) or macrophage colony stimulating factor (M-CSF) support robust infection by a recombinant EBOV (formerly Zaire EBOV) that expresses green fluorescent protein (GFP) [20] (Fig 1A). M-CSF-treated cells were consistently more permissive for EBOV infection than GM-CSF-treated cells. Consequently, M-CSF-treated macrophages were primarily investigated in these studies. We observed that M-CSF-treated peritoneal macrophages cultures that were also pretreated with a combination of IFN $\gamma$  and TNF $\alpha$  were highly resistant to EBOV infection (Fig 1A). The addition of cytokines TNF $\alpha$  and IFN $\gamma$  to macrophages has been shown to generate a proinflammatory M1 phenotype [14, 15]. Evidence that the combination of these cytokines or IFN $\gamma$  alone elicited an M1 phenotype of our isolated macrophages included significant increases in expression of proinflammatory genes such as IL-6, TNF $\alpha$ , and CXCL10 in our cells in the presence or absence of EBOV infection (S1 Fig).

Since experiments under BSL4 containment are hazardous, difficult and expensive, the BSL2 model virus, recombinant infectious vesicular stomatitis virus (rVSV) expressing EBOV GP (EBOV GP/rVSV), is frequently used to study a number of aspects of filovirus biology [21–25]. Infection of peritoneal macrophages with EBOV GP/rVSV resulted in remarkably similar effects of GM-CSF, M-CSF and the combination IFN $\gamma$ /TNF $\alpha$  treatments to that we observed with EBOV (compare Fig 1A–1B and S2 Fig). Thus, throughout these investigations, many of our studies were initially performed with EBOV GP/rVSV and subsequently confirmed and extended with EBOV in a BSL4 setting.

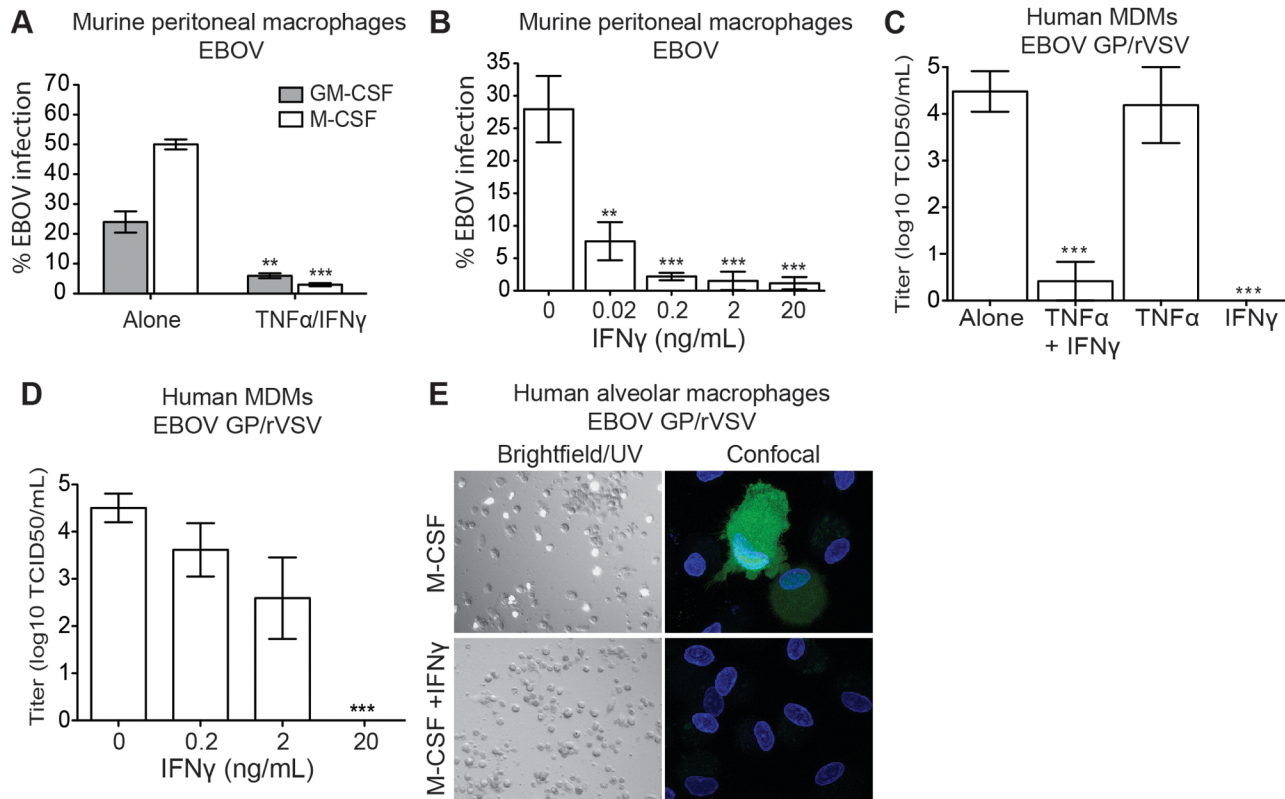


**Fig 1. IFN $\gamma$ -treated macrophages are resistant to EBOV infection.** (A) IFN $\gamma$ /TNF $\alpha$  treatment inhibits EBOV infection of BALB/c peritoneal macrophages. Cultures maintained in media containing GM-CSF or M-CSF were treated with murine IFN $\gamma$ /TNF $\alpha$  24 hours prior to EBOV-GFP infection (MOI = 0.05 in Vero E6 cells). Shown are the percent GFP positive cells at 24 hours following infection. (B) IFN $\gamma$  inhibits EBOV in a dose-dependent manner. BALB/c peritoneal macrophages were infected with EBOV-GFP (MOI = 0.05) 24 hours following IFN $\gamma$  treatment. (C) IFN $\gamma$ , but not TNF $\alpha$ , treatment of M-CSF differentiated hMDM cultures inhibits EBOV GP/rVSV infection. Virus titers were determined by end-point dilution on hMDMs from 4 independent donors. (D) Dose response curve of IFN $\gamma$  inhibition of EBOV GP/rVSV infection of M-CSF-treated hMDMs. (E) IFN $\gamma$  inhibits EBOV GP/rVSV infection in M-CSF cultured human alveolar macrophages. Left, bright field/UV (magnification: 10X). Right, confocal images (magnification: 100X). All infections were assessed 24 hours following addition of virus. Data are shown as means  $\pm$  s.e.m. Significance was determined by Student's t-test compared to no IFN $\gamma$  control, \*\* $p$  < 0.01, \*\*\* $p$  < 0.001.

doi:10.1371/journal.ppat.1005263.g001

Using EBOV GP/rVSV, we next sought to assess the relative contribution of IFN $\gamma$  and TNF $\alpha$  in inhibiting virus infection. While TNF $\alpha$  treatment of M-CSF-treated peritoneal macrophages did not inhibit EBOV GP/rVSV replication, the addition of IFN $\gamma$  prevented infection in either BALB/c or C57BL/6 peritoneal macrophages (S2 Fig). Thus, subsequent studies solely focused on the impact of IFN $\gamma$  on infection. To confirm that IFN $\gamma$ , and not TNF $\alpha$ , was important for inhibiting EBOV infection, increasing concentrations of IFN $\gamma$  were evaluated for virus inhibition. Murine IFN $\gamma$  reduced EBOV infection in a dose-dependent manner with 20 pg/mL of IFN $\gamma$  inhibiting more than 70% of infection and 2 ng/mL providing greater than 95% protection (Fig 1B).

The ability of IFN $\gamma$ , but not TNF $\alpha$ , to inhibit virus infection was also demonstrated in human macrophages. In these studies, six-day M-CSF matured human monocyte derived macrophages (hMDMs) were treated for 24 hours prior to infection with TNF $\alpha$  and/or IFN $\gamma$ . Similar to our murine macrophages findings, M-CSF-matured hMDMs were highly permissive for EBOV GP/rVSV infection and human IFN $\gamma$ , but not TNF $\alpha$ , effectively and profoundly blocked the number of cells infected by our recombinant virus (Fig 1C). In a dose-dependent manner, 200 pg/mL reduced EBOV GP/rVSV replication by about 10-fold and 20 ng/mL reduced titers

as assessed by end point dilution by more than four orders of magnitude (Fig 1D). In addition, we determined if human IFN $\gamma$  inhibits EBOV GP/rVSV infection of an *in vivo* matured macrophage population, human alveolar macrophages. These cells were isolated by bronchial lavage and phenotyped as previously described [26, 27]. Similar to the MDM cultures, M-CSF-treated cells were permissive for virus, whereas the addition of IFN $\gamma$  prevented infection of these cells (Fig 1E).

### IFN $\gamma$ inhibition requires signaling through the type II interferon receptor in mouse macrophages

IFN $\gamma$  signals through the type II IFN receptor, thereby activating JAK/STAT pathways and initiating the expression of many ISGs [28]. However, low concentrations of type I IFNs can enhance responses to type II IFN and high concentrations can inhibit [29–31]. To assess if the IFN $\gamma$  antiviral effect on macrophages was independent of type I IFN receptor signaling, peritoneal macrophages were harvested from interferon  $\alpha/\beta$  receptor knockout mice (IFNAR<sup>-/-</sup>) and cultured for 24 hours with M-CSF or M-CSF plus IFN $\gamma$  prior to EBOV GP/rVSV infection. IFN $\gamma$  treatment of BALB/c or C57BL/6 IFNAR<sup>-/-</sup> macrophages inhibited virus infection (S3A and S3B Fig), indicating that IFN $\gamma$  does not require the presence of a functional type I IFN receptor for its antiviral effect. To verify that the IFN $\gamma$  response required the type II receptor, C57BL/6 IFN $\gamma$  receptor knockout (IFN $\gamma$ R<sup>-/-</sup>) peritoneal macrophages were harvested and stimulated with M-CSF or M-CSF plus IFN $\gamma$  prior to infection. As expected, IFN $\gamma$  treatment had no effect on EBOV GP/rVSV viral titers in IFN $\gamma$ R<sup>-/-</sup> cells, indicating that the type II IFN receptor is required for IFN $\gamma$ -mediated inhibition of virus infection (S3C Fig).

While studies above indicated that IFN $\gamma$  blocked EBOV and EBOV GP/rVSV infection of macrophages from wild-type mice, EBOV GP/rVSV infection of these cells was modest and virus spread in these cultures was not observed. In contrast, macrophages from BALB/c or C57BL/6 IFNAR<sup>-/-</sup> mice were highly permissive to EBOV GP/rVSV and IFN $\gamma$  treatment of these cells profoundly decreased infection in a dose dependent manner (S3A and S3B Fig). Hence, we used peritoneal macrophages from IFNAR<sup>-/-</sup> mice in subsequent studies with EBOV GP/rVSV.

### IFN $\gamma$ inhibition of EBOV RNA levels in infected mouse macrophages

To identify the step(s) of the virus life cycle that is/are blocked by IFN $\gamma$ , BALB/c IFNAR<sup>-/-</sup> peritoneal macrophages were treated with IFN $\gamma$  for 24 hours, infected with EBOV GP/rVSV, and monitored for viral RNA accumulation via qRT-PCR. After 2 hours of infection, IFN $\gamma$  treatment had no significant effect on the quantity of VSV matrix (M) or polymerase (L) RNA detected, suggesting that IFN $\gamma$  does not affect early events in the life cycle, such as entry (Fig 2A). A previous study supports this observation, as IFN $\gamma$  treatment of differentiated hMDMs did not significantly reduce entry of EBOV viral-like particles (VLPs) [32]. However, by 6 and 24 hours after infection, the steady increase in VSV M and L RNA levels in infected M-CSF-stimulated peritoneal macrophages was significantly reduced by IFN $\gamma$  treatment (Fig 2A).

Gene expression of *Mononegavirales* viruses, including filoviruses and rhabdoviruses, is initiated by primary transcription of mRNAs that does not require new viral protein synthesis [33]. However, subsequent viral genome replication requires viral protein production and replication of the genome is blocked by inhibitors of protein synthesis such as cycloheximide (CHX) [34]. Therefore, to narrow down which step(s) within the life cycle is affected by IFN $\gamma$ , we compared the ability of IFN $\gamma$  and CHX to inhibit viral RNA production and determined if the combination of these two drugs inhibited viral RNA levels to a greater extent. BALB/c IFNAR<sup>-/-</sup> peritoneal macrophages were treated with M-CSF in the presence or absence of IFN $\gamma$

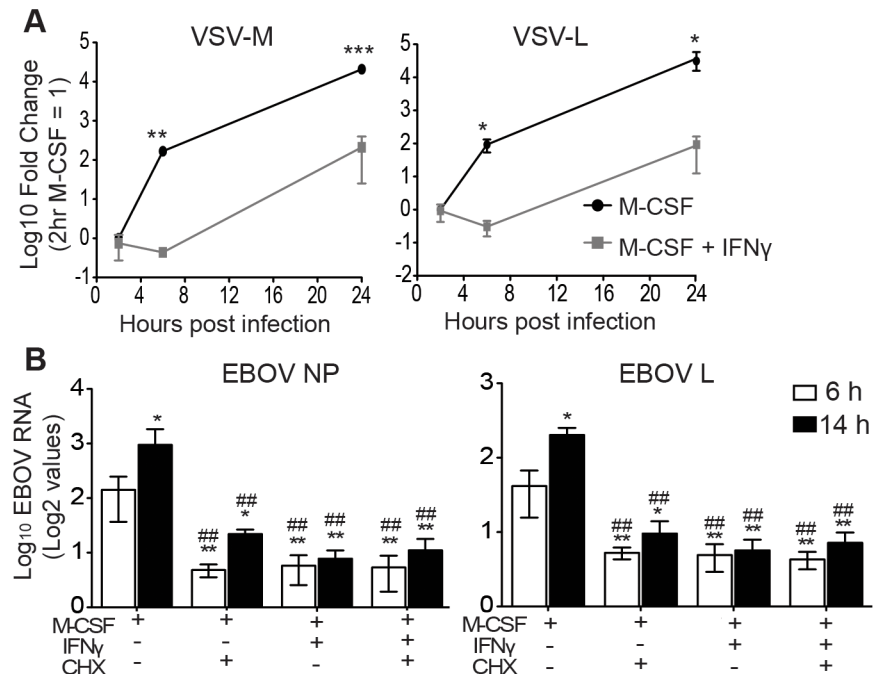


**Fig 2. IFN $\gamma$  blocks EBOV GP/rVSV and EBOV RNA synthesis.** (A) M-CSF cultured peritoneal macrophages pre-treated for 24 hours with IFN $\gamma$  have decreased EBOV GP/rVSV RNA synthesis at 6 and 24 hours following infection. Total RNA from IFN $\gamma$ -treated or untreated peritoneal macrophages at indicated time points was assessed by qRT-PCR for VSV matrix (M) and polymerase (L) RNA. Log<sub>2</sub> value of 2 hour M-CSF alone = 1 and data is shown as Log<sub>10</sub> of the fold change. Significance was determined by one sample t-test compared to 2 hour M-CSF only control. \* $p < 0.05$ , \*\* $p < 0.01$ , \*\*\* $p < 0.001$ . (B) IFN $\gamma$  treatment decreases EBOV RNA levels to the same extent as the protein synthesis inhibitor cycloheximide. Total RNA isolated at 6 or 14 hours following EBOV infection of M-CSF cultured peritoneal macrophages treated with or without IFN $\gamma$  and/or CHX was quantified by qRT-PCR for EBOV nucleoprotein (NP) and polymerase (L) RNA. Data is shown as log<sub>2</sub> values. Significance was determined by ANOVA with a Tukey post-test. \* $p < 0.05$ , \*\* $p < 0.01$  (compared to 6 hours M-CSF alone). ## $p < 0.01$  (compared to 14 hours M-CSF alone). ns, not significantly different.

doi:10.1371/journal.ppat.1005263.g002

for 24 hours. At the initiation of EBOV infection under BSL4 conditions, CHX was added and viral RNA levels were assessed at 6 and 14 hours of infection. CHX or IFN $\gamma$  suppressed EBOV nucleoprotein (NP) and polymerase (L) RNA levels equally and the combination of inhibitors did not further reduce EBOV RNA production (Fig 2B). Similar results were observed with EBOV GP/rVSV infections harvested at 6 hours (S4 Fig). In total, these findings indicate that IFN $\gamma$  treatment interferes with RNA synthesis that is dependent upon protein synthesis and suggests that virus replication is blocked.

### Human macrophage gene arrays identify novel IFN $\gamma$ -stimulated genes that inhibit EBOV infection

Type I or type II IFN treatment of macrophages elicits expression of hundreds of IFN stimulated genes (ISGs) and suppresses the expression of an additional smaller group of genes. Production of ISG proteins alters macrophage function and protects cells from viral infection [35]. While gene sets activated by these two types of IFNs overlap, both type I and II IFNs also stimulate unique subsets of genes [17, 18, 36]. To determine the impact of IFN $\gamma$  stimulation on gene expression in our macrophage cultures, we performed microarray analyses. We identified 268 genes with at least two-fold increased or decreased expression in IFN $\gamma$ -treated six-day-

M-CSF-matured hMDM (Fig 3A and S1 Table). In parallel, gene arrays were performed in IFN $\gamma$ -treated alveolar macrophages and 45 genes were identified to have altered expression (S5 Fig and S2 Table). Forty-one of the significantly altered genes were identified in both arrays (Fig 3B and S6A Fig). Through pathway analysis of the gene profiles, we discovered that the top IFN $\gamma$ -upregulated genes in our arrays are involved in immune responses, development, signal transduction, ATP metabolism, or transcription (S6B Fig).

Our arrays identified IFN $\gamma$ -enhanced expression of ISGs known to be primary-response genes, such as the transcription factors IRF1 and IRF9, and more poorly studied secondary-response ISGs, such as the p65 GBPs and the apolipoprotein L family of proteins that are thought be regulated by IRFs [37]. Consistent with previous reports, a number of chemokines

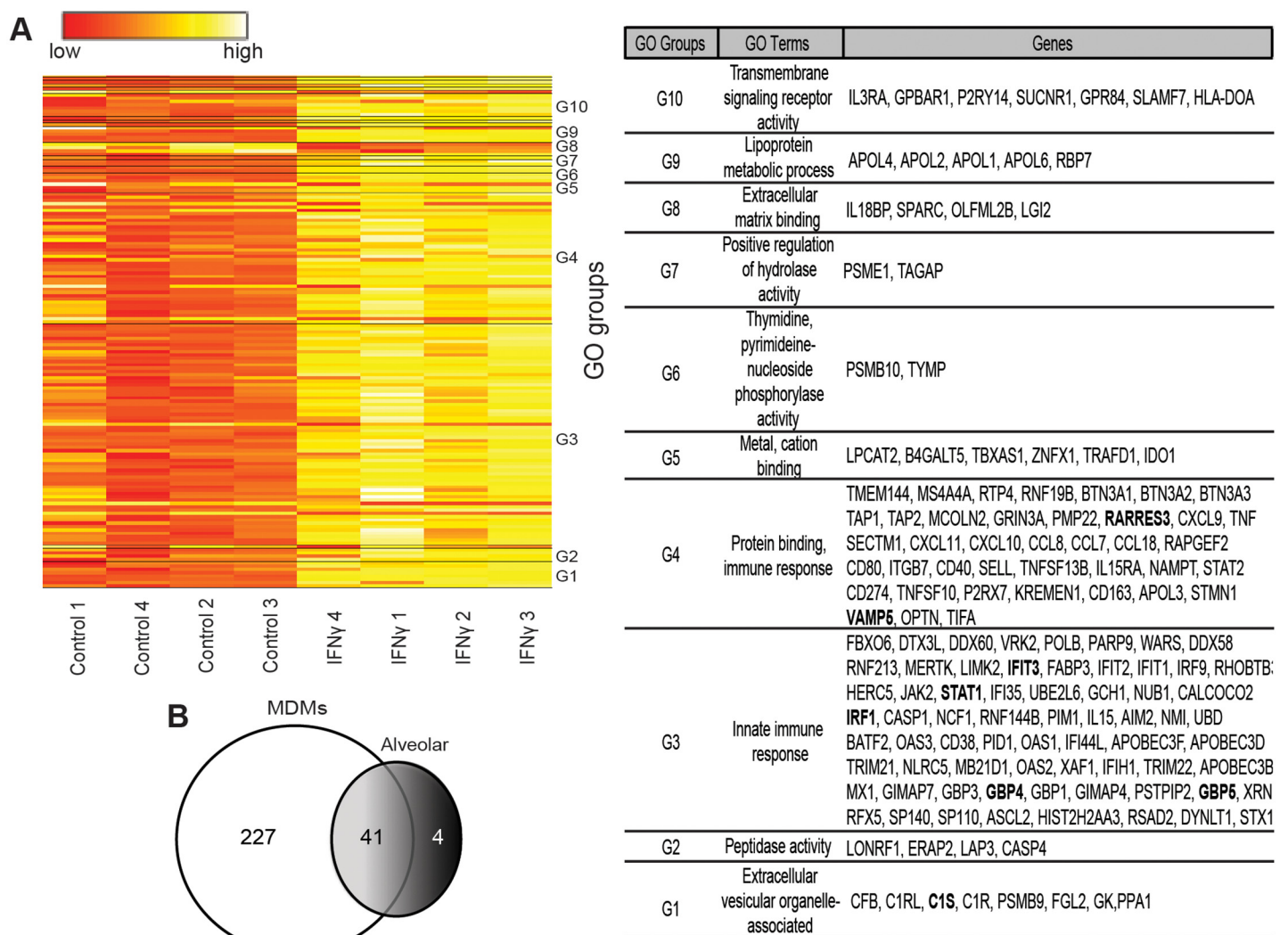


**Fig 3. Human MDM gene expression is altered by 24 hours of IFN $\gamma$  treatment.** M-CSF cultured hMDMs were incubated with or without IFN $\gamma$  for 24 hours and RNA was harvested for gene arrays. (A) Heat map summaries of hMDM gene expression significantly altered by IFN $\gamma$ . Human MDMs were obtained from four different volunteers and treated with M-CSF or M-CSF plus IFN $\gamma$ . Genes were clustered into annotated ontology groups and listed in the corresponding GO groups table with their respective GO terms. Significance was determined by paired t-test analysis with cutoff values of at least two-fold change and  $p < 0.01$ . NUSE analysis of the array demonstrated that the means were centered at a value of 1 and minimum and maximum values between 0.95 and 1.05. ISGs that were assessed further in this study are bolded in the GO table. (B) Venn diagram representing the statistically significant individual and shared genes altered by IFN $\gamma$  in hMDMs and human alveolar macrophages.

doi:10.1371/journal.ppat.1005263.g003

(CXCL9, CXCL10, CCL8 and CXCL11) and complement components (C1s and C1r) were also highly upregulated by IFN $\gamma$  [14, 16, 17, 38]. Our array findings were validated by examining mRNA levels of several of the top ISGs, including IRF1, GBP4, GBP5, IFIT3, RARRES3, and VAMP5 by qRT-PCR (Fig 4A and S5B Fig).

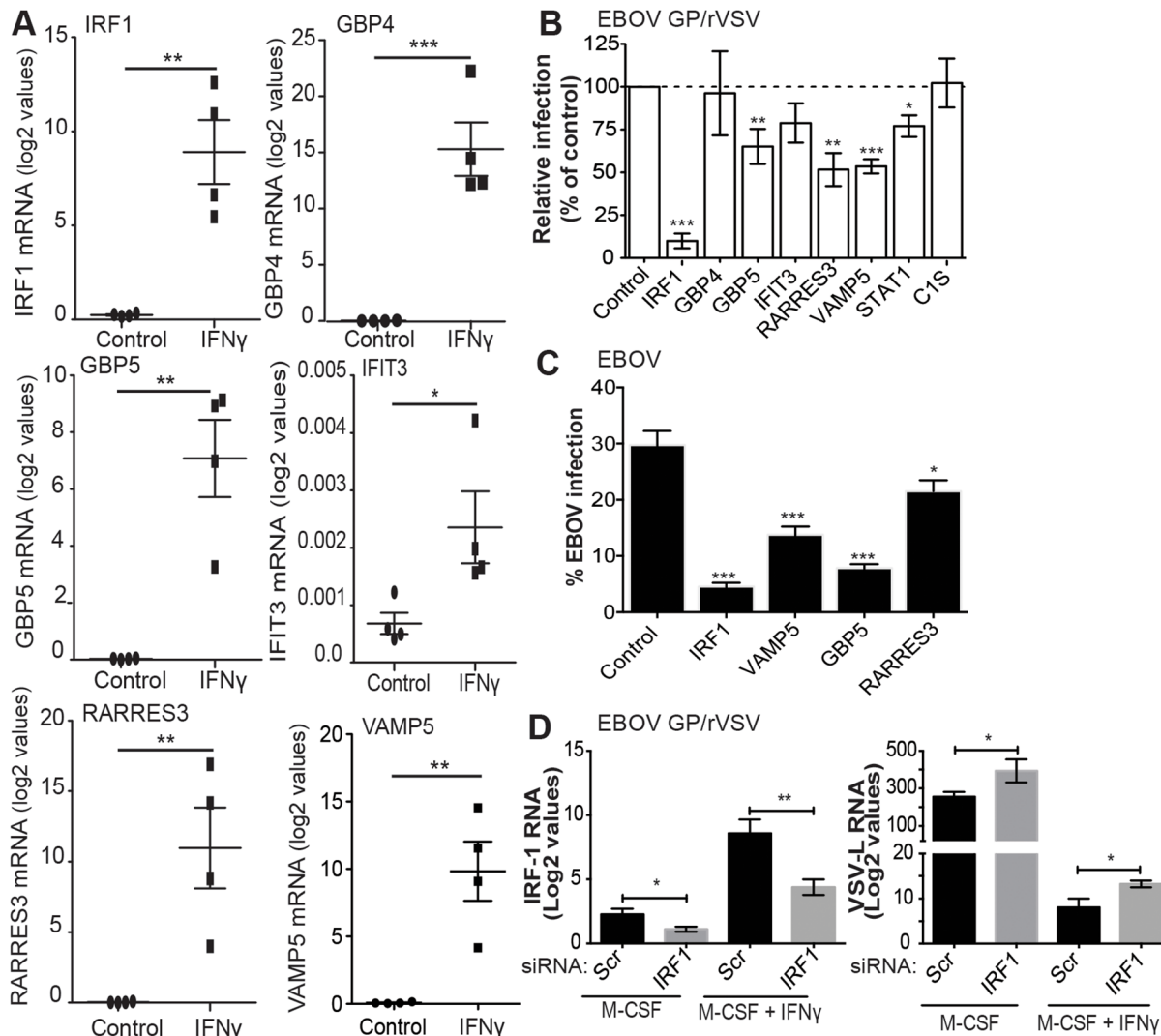


**Fig 4. Identification of IFN $\gamma$ -stimulated genes that inhibit EBOV infection.** (A) mRNA validation of hMDM profiling results for several of the top IFN $\gamma$ -stimulated genes identified in our gene arrays. RNA obtained for the microarray analysis was assessed for mRNA levels of the selected genes by qRT-PCR. Results are represented as the log2 values. (B) Identification of IFN $\gamma$ -stimulated genes that inhibit EBOV GP/rVSV infection. Highly permissive HEK 293T cells stably expressing TIM -1 (H3 cells) were infected with EBOV GP/rVSV 48 hours following transfection of 2  $\mu$ g of ISG-RFP lentiviral constructs. Cells gated for RFP expression were assessed for EBOV GP/rVSV infection by detection of GFP. Shown is infection of EBOV GP/rVSV in ISG expressing cells relative to infection of cells transfected with a fluc-RFP expressing lentivirus (control). (C) Novel ISGs that inhibit EBOV GP/rVSV also block EBOV infection. HeLa cells were infected with EBOV 48 hours following electroporation of 5  $\mu$ g of ISG-RFP lentiviral constructs. Infection was assessed by microscopy 24 hours later and percent of cells that were GFP positive were calculated by CellProfiler image analysis software. A lentiviral construct expressing IRF1 served as a positive control in these studies. (D) IRF1 knock down increases EBOV GP/rVSV infection following IFN $\gamma$  stimulation. IRF1 or scrambled (Scr) siRNA were loaded into HEK 293T derived exosomes. SiRNA loaded exosomes (2.5  $\mu$ g) were delivered and IFN $\gamma$  added to BALB/c IFNAR $^{-/-}$  peritoneal macrophages 24 hours prior to EBOV GP/rVSV infection (MOI = 0.1). Twenty-four hours following infection, total RNA was isolated from the macrophages. Amount of IRF1 expression and infection (by detection of VSV polymerase (L)) was quantified by qRT-PCR. Results represent the means  $\pm$  s.e.m. Significance was determined by Student's t-test analysis, \* $p$  < 0.05, \*\* $p$  < 0.01, \*\*\* $p$  < 0.001.

doi:10.1371/journal.ppat.1005263.g004

To assess the importance of some of our most significantly upregulated ISGs in controlling EBOV GP/rVSV and EBOV infection, IFN $\gamma$ -upregulated genes were transfected into cells and their effect on virus infection was assessed. The panel of ISGs included both well-studied and poorly characterized IFN $\gamma$ -responsive genes. Eight lentiviral constructs that expressed an ISG and red fluorescent protein (RFP) were assessed for inhibition of EBOV GP/rVSV or EBOV in highly permissive cells [23].

Transfection of the construct expressing IRF1 strongly inhibited EBOV GP/rVSV and EBOV replication, as has been previously shown for positive strand and other negative strand RNA viruses (Fig 4B and 4C) [39, 40]. As IRF1 is a transcription factor critical for IFN $\gamma$  signaling by driving downstream expression of many IFN $\gamma$  target genes [19], we also assessed if knock down of IRF1 in M-CSF-treated and M-CSF/IFN $\gamma$ -treated macrophages altered infection of EBOV GP/rVSV in peritoneal macrophages. IRF1 siRNA or scrambled control siRNA was delivered to peritoneal macrophages by exosomes since direct siRNA transfection of macrophages is highly inefficient. To validate this siRNA delivery method, we initially demonstrated that exosomes are efficiently engulfed by murine peritoneal macrophages (S7 Fig). In the context of EBOV GP/rVSV infection, delivery of IRF1 siRNA containing exosomes knocked down IRF1 mRNA levels by approximately 50% in both M-CSF- and M-CSF/IFN $\gamma$ -treated macrophages (Fig 4D). With IRF1 knock down, a significant increase in EBOV GP/rVSV RNA was observed 24 hours following infection, consistent with the importance of IRF1 expression in controlling virus infection by IFN $\gamma$ .

Additional less well-characterized ISGs that were highly upregulated in our gene array studies were also assessed for their ability to directly control virus infection. Ectopic expression of GBP5, RARRES3 and VAMP5 resulted in significant inhibition of EBOV GP/rVSV (Fig 4B). Evaluation of these ISGs for their ability to inhibit EBOV demonstrated that they also effectively blocked EBOV, identifying these as novel ISGs that are likely important for the control of EBOV in IFN $\gamma$ -treated cells. Surprisingly, expression of STAT1 only modestly inhibited EBOV GP/rVSV infection, likely because significant levels of STAT1 are constitutively expressed within these cells and control of STAT1 activity is primarily regulated by its phosphorylation status [41–43]. Certainly not all ISGs tested that were highly upregulated in our gene arrays inhibited virus replication; GBP4, IFIT3, IFI27 and C1S had no effect on EBOV GP/rVSV.

### *In vivo* IFN $\gamma$ treatment protects IFNAR<sup>-/-</sup> mice against lethal EBOV GP/rVSV challenge, but is less efficacious against wild-type VSV

Since IFN $\gamma$  robustly inhibits EBOV GP/rVSV and EBOV infection of macrophages and macrophages are an important cellular target for filoviruses pathogenesis, we evaluated the ability of intraperitoneally (i.p.) administered IFN $\gamma$  to protect mice against lethal i.p. challenge. For these studies, BALB/c IFNAR<sup>-/-</sup> mice were used as little to no pathogenesis is observed with EBOV GP/rVSV infections of wild-type mice, but significant morbidity and mortality occurs in IFNAR<sup>-/-</sup> mice. Initial IFN $\gamma$  dose response studies demonstrated that both 3.3 and 10  $\mu$ g of IFN $\gamma$  protected IFNAR<sup>-/-</sup> mice against lethal EBOV GP/rVSV challenge (S8A Fig). Further, neither dose of IFN $\gamma$  had any detectable consequence on the weight or health of the mice. Therefore, subsequent studies were performed with both dosages. IFN $\gamma$  administered by i.p. injection 24 hours prior to, 2 or 6 hours after a lethal dose of EBOV GP/rVSV protected mice against challenge, with treated mice demonstrating significantly reduced mortality, weight loss and clinical sickness scores compared to untreated, virus-infected animals (Figs 5A and S8B–S8D). At the 10  $\mu$ g IFN $\gamma$  dose, we also assessed survival of mice when IFN $\gamma$  was given at 12 and 48 hours after challenge. While only 75% of the mice survived challenge in the 12-hour post challenge group, the protection offered by this treatment was not statistically different than

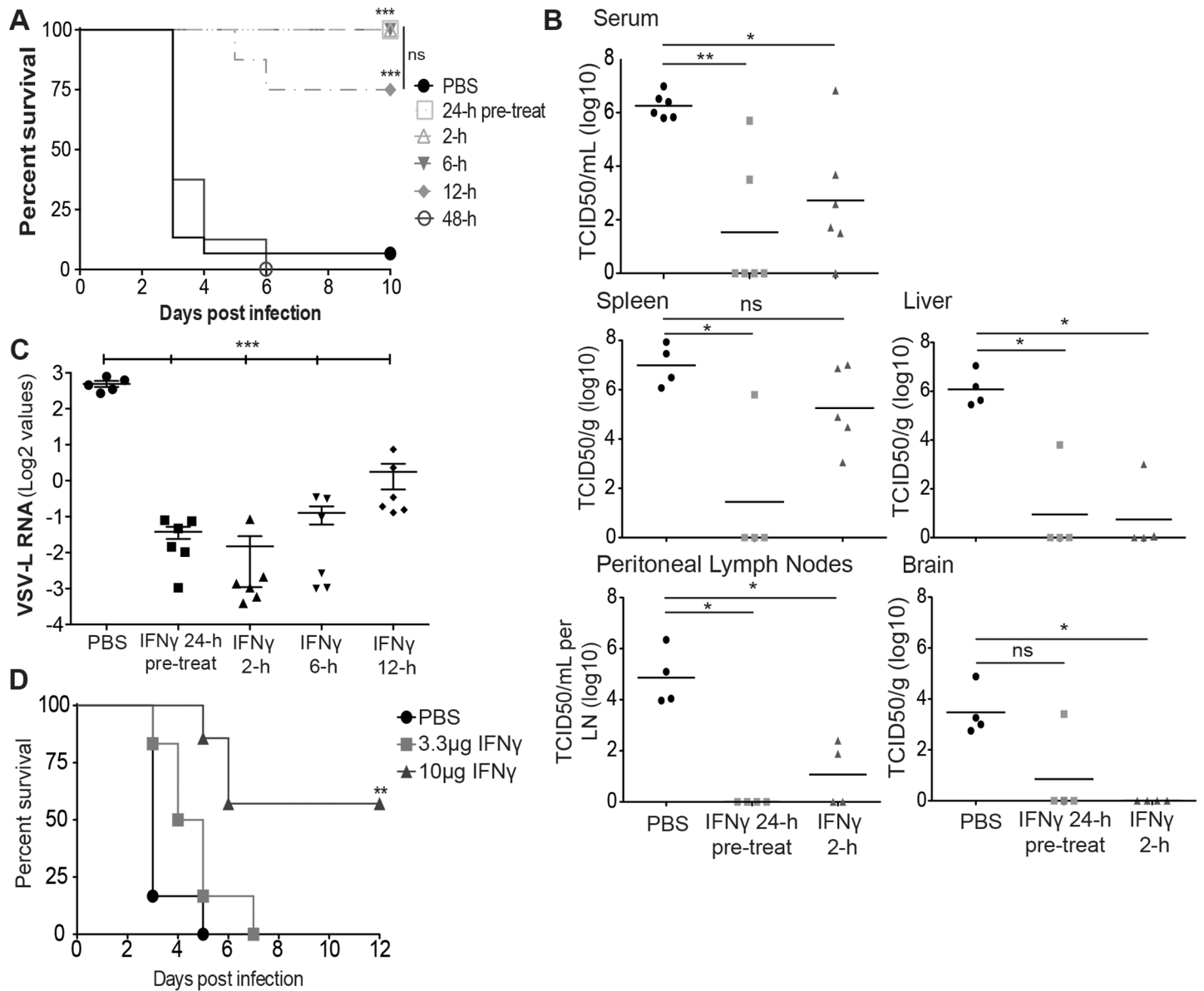


**Fig 5. IFN $\gamma$  reduces EBOV-GP/rVSV morbidity and mortality.** (A) IFN $\gamma$  enhances survival of EBOV GP/rVSV infected mice. IFN $\gamma$  (10  $\mu$ g) or PBS was administered by i.p. injection to BALB/c IFNAR<sup>-/-</sup> mice 24 hours prior to or 2, 6, 12 or 48 hours following EBOV GP/rVSV infection ( $n \geq 8$ /treatment). (B) IFN $\gamma$  treatment as a 24 hour pre-treatment or a 2 hour post-treatment reduces serum viremia and organ titers of EBOV GP/rVSV-infected mice. Sera and organs were harvested at 48 hours following infection ( $n \geq 4$ /treatment) in mice treated with 3.3 $\mu$ g of IFN $\gamma$ . Viremia and organ virus titers were determined by endpoint dilution of serum or homogenized organ samples on Vero cells. Significance was calculated by Mann-Whitney test compared to PBS control, \* $p < 0.05$ , \*\* $p < 0.01$ . ns, not significant. (C) Intraperitoneal IFN $\gamma$  treatment of mice significantly inhibits EBOV GP/rVSV infection of peritoneal cells. Peritoneal cells were isolated from EBOV GP/rVSV infected mice treated with 3.3 $\mu$ g of IFN $\gamma$  at times noted prior to or following challenge. Amount of VSV-L RNA was determined by qRT-PCR. Significance was determined by ANOVA with a Tukey post-test, \*\*\* $p < 0.001$ . (D) Intramuscular administration of IFN $\gamma$  increases survival of IFNAR<sup>-/-</sup> mice. PBS or IFN $\gamma$  at the indicated concentration was administered by i.m. injection 24 hours prior to i.p. injection of EBOV GP/rVSV. For A & D, significance was determined by Mantel-Cox Test, \*\* $p < 0.01$ , \*\*\* $p < 0.001$ .

doi:10.1371/journal.ppat.1005263.g005

that conferred at time points more proximal to the challenge (Fig 5A). However, IFN $\gamma$  administered 48 hours following EBOV GP/rVSV did not protect mice against lethal challenge.

Consistent with reduced morbidity and mortality in the EBOV GP/rVSV infected, IFN $\gamma$ -treated mice, mice treated with 3.3  $\mu$ g of IFN $\gamma$  at 24 hour before infection had dramatically

lower EBOV GP/rVSV viremia at day 2 of infection (Fig 5B). Little to no detectable viral load was observed in liver, peritoneal lymph nodes or brain, of the pre-treated mice with somewhat higher levels of virus present in the spleen. Similar trends were observed in mice treated with IFN $\gamma$  2 hours following EBOV GP/rVSV infection (Fig 5B), but splenic virus loads were higher in these mice, suggesting that some virus had trafficked to the spleen by 2 hours following inoculation. Nonetheless, IFN $\gamma$  treatment still controlled virus titers in other organs.

To assess the impact of IFN $\gamma$  treatment on cells at the site of infection, peritoneal cells were isolated 24 hours following EBOV GP/rVSV infection of untreated or IFN $\gamma$ -treated mice. IFN $\gamma$  treated peritoneal cells had reduced viral RNA levels compared to infected, PBS-treated control cells, regardless of whether IFN $\gamma$  was given 24 hours prior to, 2, 6 or 12 hours following challenge. These findings suggest that active infection at the site of challenge is ongoing at 24 hours following infection and that IFN $\gamma$  administration either before or at early time points following infection is able to profoundly reduce virus load at the site of virus challenge (Fig 5C).

As a control for these studies, we also evaluated the ability of IFN $\gamma$  to protect against wild-type VSV infection. Initial studies demonstrated that equivalent concentrations of VSV were more virulent in mice than our recombinant virus, EBOV GP/rVSV, perhaps because of the broad cellular tropism conferred by the native VSV glycoprotein G [44, 45]. As a consequence, in these studies we used  $10^2$  infectious units of VSV as our challenge virus, the lowest concentration of VSV that resulted in predictable death. IFNAR $^{-/-}$  mice challenged with VSV were given 3.3  $\mu$ g of IFN $\gamma$  either 24 hours prior or 2 hours after challenge. While the 24-hour pre-treated mice had significant protection, 40% mortality was still observed. Surprisingly, the survival of the 2-hour IFN $\gamma$  post-treatment mice was not significantly different from the PBS-treated, VSV infected mice (S8B Fig). This finding stands in contrast to the robust protection IFN $\gamma$  conferred at 2, 6 and 12 hours following EBOV GP/rVSV challenge. These findings suggested that VSV infection is less sensitive to IFN $\gamma$ , particularly when administered as a post-challenge antiviral.

Previous studies have demonstrated that IFN $\gamma$  treatment administered by intramuscular (i.m.) injection allows for slower release and an extended half-life of the drug [46]. Further, this injection route is utilized in many clinical therapeutics. Thus, we investigated the ability of this administration route to protect mice against lethal EBOV GP/rVSV. Mice given 10  $\mu$ g of IFN $\gamma$  by i.m. injection 24 hours prior to EBOV GP/rVSV infection significantly protected against lethal challenge (Fig 5D).

## IFN $\gamma$ protects mice from lethal EBOV challenge

Based on the promising results we observed with IFN $\gamma$  protection of EBOV GP/rVSV infected mice, we next sought to determine the ability of IFN $\gamma$  to protect mice from lethal challenge with mouse-adapted EBOV (MA-EBOV). BALB/c mice were administered 3 or 10  $\mu$ g of IFN $\gamma$  i.p. and challenged i.p. with MA-EBOV 24 hours later. Initial IFN $\gamma$  dose response studies indicated that mice pretreated with 10  $\mu$ g of IFN $\gamma$  were better protected against MA-EBOV than treatment with 3  $\mu$ g (S9A Fig). Thus, in subsequent studies, mice challenged with MA-EBOV were administered 10  $\mu$ g of IFN $\gamma$ . Since IFN $\gamma$  given 48 hours following infection did not protect IFNAR $^{-/-}$  mice against EBOV GP/rVSV (Fig 5A), in these studies we assessed the protection IFN $\gamma$  conferred against MA-EBOV when administered 24 hours prior to, at the time of infection, 6 or 24 hours following infection. All IFN $\gamma$ -treated mice, regardless of time of treatment, had significantly less morbidity and mortality than untreated, infected mice, with treatment as late as 24 hours following infection protecting 100% of the mice from death (Fig 6A and 6B). Lower MA-EBOV viremia levels were observed in the 24 hour post challenge treated mice, but

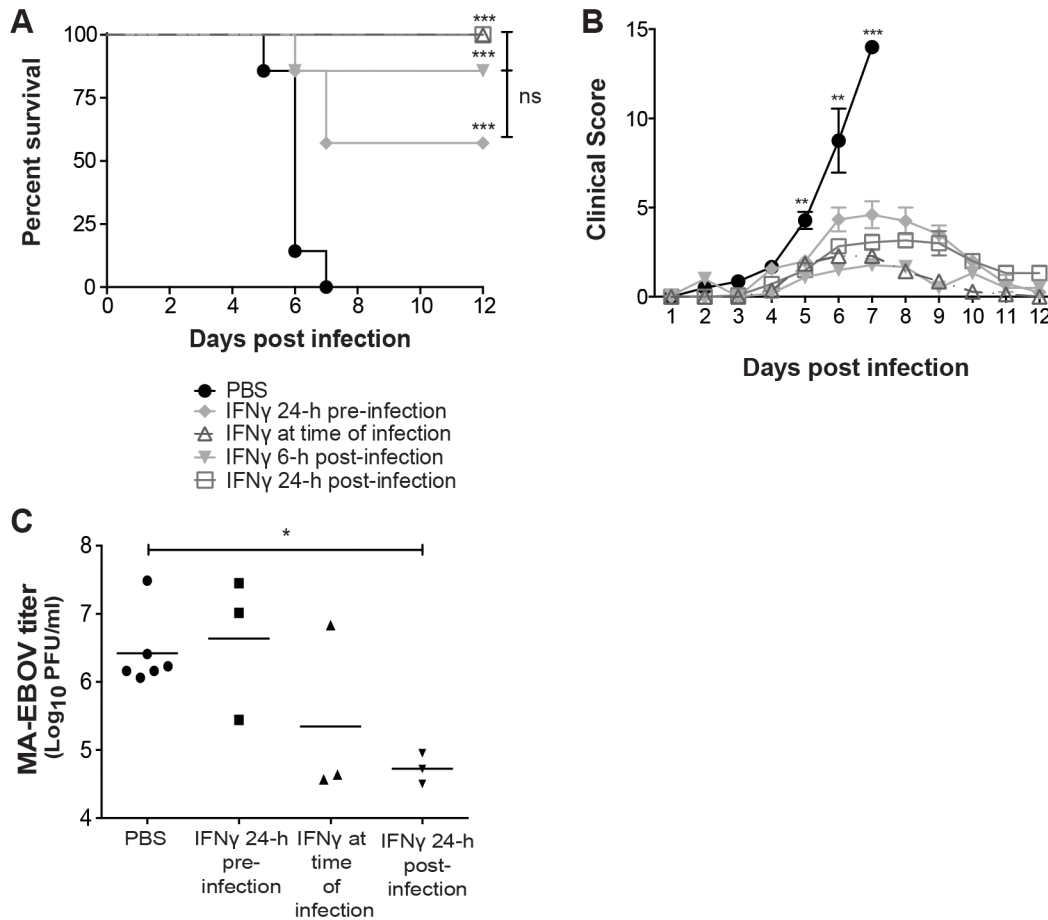


**Fig 6. IFN $\gamma$  protects mice from EBOV morbidity and mortality.** (A) IFN $\gamma$  protects mice from lethal MA-EBOV infection. IFN $\gamma$  (10  $\mu$ g) or PBS was administered by i.p. injection to BALB/c mice 24 hours prior to, at the time of infection, 6 or 24 hours following infection ( $n \geq 7$ /treatment). Significance was determined by Mantel-Cox Test,  $**p < 0.01$ ,  $***p < 0.001$ . ns, not significantly different. (B) IFN $\gamma$  treatment reduces MA-EBOV morbidity. Results represent mean clinical sickness scores  $\pm$  s.e.m ( $n \geq 7$ /treatment). Significance was determined by Student's t-test compared to PBS control. (C) IFN $\gamma$  treatment significantly reduces MA-EBOV viremia in mice treated 24 hours following infection. Serum was collected 4 days following infection ( $n = 3-6$  mice/treatment) and serial dilution of sera on Vero-E6 cells to assess plaques formed determined viremia titers. Results represent means  $\pm$  s.e.m. Significance was determined by Mann-Whitney test compared to PBS control,  $*p < 0.05$ .

doi:10.1371/journal.ppat.1005263.g006

not in the 24 hour pre-infection treatment group, suggesting that IFN $\gamma$  administration as a post-exposure antiviral may prove more efficacious than when used prophylactically (Fig 6C).

## Discussion

Our results are the first to demonstrate the ability of IFN $\gamma$  to protect animals both prophylactically and therapeutically against EBOV infection and suggest that this FDA-approved drug may be a useful antiviral for individuals with recent high-risk exposure. IFN $\gamma$  treatment profoundly inhibited EBOV infection of peritoneal macrophages in tissue culture, consistent with the protection conferred by IFN $\gamma$  and evidence that this cell type is an important early target for virus replication. Since antiviral efficacy required the presence of IFN $\gamma$  receptor, but not the type I receptor, IFN $\gamma$  control of EBOV infection occurs independently of type I IFN responses. Thus, we sought to identify specific IFN $\gamma$ -stimulated genes involved in its antiviral effect. In addition to previously characterized ISGs, we identified three novel IFN $\gamma$ -stimulated factors, GBP5, RARRES3 and VAMP5. To date, GBP5, RARRES3 or VAMP5 has not been shown to

control negative strand RNA virus infection. Finally, we demonstrated that the recombinant BSL2-level virus, EBOV GP/rVSV, recapitulates our findings with EBOV, arguing that studies with this BSL2 model virus may serve as a safer and cost effective alternative for initial evaluations of novel anti-filoviral agents.

Antiviral activity conferred by IFN $\gamma$  against members of the *Mononegavirales* has been previously reported. For instance, addition of *Pteropus alecto* IFN $\gamma$  to bat cells protects against the paramyxoviruses, Semiki forest virus and Hendra virus [47]. Additionally, several lines of evidence indicate that IFN $\gamma$  is effective against rabies virus in tissue culture and *in vivo*, potentially through stimulation of type I IFN pathways [48, 49].

Our studies also suggest that IFN $\gamma$  treatment does not specifically target EBOV, as it protected against our BSL2 recombinant virus EBOV GP/rVSV and, to a more modest degree, against VSV in mice lacking type I IFN signaling. However, the timing of IFN $\gamma$  protection against wild-type EBOV and wild-type VSV differed. IFN $\gamma$  treatment protected against VSV only when given prior to infection, whereas post-challenge treatment appeared somewhat more efficacious against EBOV than pre-challenge treatment. Recent studies demonstrate that some ISGs are solely synthesized during the first few hours following IFN stimulation, whereas others are expressed for longer periods of time [50]. The difference in timing of IFN $\gamma$  protection against VSV versus EBOV suggests that ISGs responsible for protection may differ. Future studies are needed to explore this possibility. Since mice challenged with EBOV GP/rVSV were protected by IFN $\gamma$  treatment at post challenge time points in a manner similar to EBOV, the difference in timing of protection may be related to the cell populations targeted by the two wild-type viruses.

Our studies have only begun to identify IFN $\gamma$ -stimulated proteins that contribute to the control of EBOV infection. Studies with type I IFNs have shown that a subset of ISGs preferentially target negative strand RNA viruses [51] and this may be the case with IFN $\gamma$ -stimulated ISGs as well. Not surprisingly, expression of IFN $\gamma$ -activated transcription factor IRF1 inhibited EBOV infection and this ISG served as a positive control in these experiments [18, 40, 52]. Other downstream ISGs were selected for study based on the enhancement of their expression elicited by IFN $\gamma$  in our gene array studies and availability of expression constructs. The ability of GBP5, RARRES3 and VAMP5 to inhibit negative strand RNA viruses has been poorly studied and the mechanisms driving inhibition of virus replication remain to be elucidated. Each of these ISGs reduced EBOV infection; however, as has been shown with other viruses, combinations of ISGs are likely to provide additive or even synergistic inhibition if the ISGs are targeting independent modulatory pathways [40].

We also demonstrated that knockdown of IRF1 could modestly rescue EBOV GP/rVSV infection in peritoneal macrophages that were stimulated with IFN $\gamma$ . GBP5, RARRES3 and VAMP5 all contain predicted IRF1 binding sites based on analysis of their genomic sequence with the UCSF genome browser. In addition, a recent study demonstrated that murine IRF1<sup>-/-</sup> bone-marrow derived macrophages have significantly decreased GBP5 gene expression compared to WT cells following *Francisella novicida* infection [53]. Together, these observations suggest IRF1 transcriptional stimulation may control expression of these novel ISGs that in turn participate in control of EBOV infection.

Our identification of IFN $\gamma$ -elicited ISGs that inhibit EBOV infection adds to the ISGs that are identified to target this virus. To date, a limited number of ISGs has been identified to restrict EBOV infection, including tetherin, ISG15, RIG-I, STAT1 and STAT2 [54–59]. Additionally, IFITM1 has been identified to inhibit EBOV entry. This ISG blocks EBOV GP-dependent entry [60]. Interestingly, in our studies, IFITM1 expression was not significantly upregulated in IFN $\gamma$ -stimulated macrophages. Consistent with this, we did not see an IFN $\gamma$ -dependent impact on total viral RNA present in cells at early times during infection (2 hours),

suggesting very early events are not affected by IFN $\gamma$  treatment. Consistent with this, a previous study demonstrated that IFN $\gamma$  does not affect EBOV GP-dependent entry [32].

IFN $\gamma$  reduced viral RNA levels in a manner similar to that observed with the protein synthesis inhibitor, cycloheximide, suggesting that IFN $\gamma$  inhibits one or more viral life cycle events at or downstream of translation. ISGs have previously been identified to block viral protein translation, including the oligoadenylate synthetases [61] and indoleamine 2,3-dioxygenase [62]; however, to date, none of these has been assessed for their ability to inhibit EBOV replication. Expression of both of these ISGs was significantly increased in our IFN $\gamma$ -stimulated macrophages and likely contributed to the inhibition of EBOV infection that we observed.

IFN $\gamma$  is produced by several different hematopoietic cell types including natural killer cells, natural killer T cells and T lymphocytes [63, 64]. IFN $\gamma$  induces specific cytotoxic and antiviral immunity by direct ISG production and through indirect mechanisms that likely provide additional mechanisms of action benefiting its clinical profile [19]. These added effects include IFN $\gamma$  assisting in the activation of the adaptive immune system. IFN $\gamma$ /receptor interactions lead to the up-regulation of phagocytosis, antigen processing and presentation in DCs and macrophages driving production of the Th1 phenotype of CD4+ T cells [19]. The relative importance of each of this diverse array of downstream effects on EBOV infection still needs to be elucidated.

EBOV evades the host innate immune signaling pathways through impaired type I and type II IFN signaling, dysregulated proinflammatory cytokine expression and suppression of DC maturation and T-cell activation [65–67]. This immune dysregulation is thought to allow EBOV to gain the upper hand during the course of infection; however, a reduction in viral antigen by as little as 2-fold appears to be the difference between the host survival and death during EBOV infection [68, 69]. As our IFN $\gamma$  treatment of EBOV infected mice as late as 24 hours following lethal challenge demonstrates effective control of viral load, IFN $\gamma$  treatment likely assists in overcoming EBOV-induced impairment of immune function by activation and maturation of immune cells as well as eliciting ISGs, leading to reduced EBOV RNA production as well as perhaps innate immune control of other aspects of the EBOV life cycle.

Filovirus pathogenesis has been investigated through the use of a variety of different animal models, including mice, guinea pigs, hamsters, and non-human primates (NHPs) [70–72]. These various model organisms offer different advantages for studying EBOV pathogenesis and assessing novel antiviral treatments. While NHPs are considered the most representative model for EBOV infection as they display very similar symptoms to those observed in humans [72], they are expensive and, ethically, the use of these animals should be limited to late phase pre-clinical studies. In contrast, infection of mice with MA-EBOV serves as a good, genetically manipulatable small animal model for early phase evaluation of vaccines and therapeutic interventions, allowing assessment of their impact on viral pathogenesis. Our definitive evidence of IFN $\gamma$  efficacy in this small animal model paves the way for future NHP studies to further assay the anti-EBOV properties of IFN $\gamma$ .

These *in vivo* studies suggest that IFN $\gamma$  may serve as an effective prophylactic and/or therapeutic drug against EBOV infection. Several different IFNs are currently FDA approved to treat a variety of infections and autoimmune disorders. Type I IFNs have been used clinically as therapeutics against both hepatitis B and C infections [73, 74], but showed mixed efficacy against EBOV infection in NHPs [11–13]. The antiviral effects of IFN $\gamma$  are less well-studied, but this protein is a FDA-approved therapy for chronic granulomatous disease and osteopetrosis [75, 76]. Chronic granulomatous patients receive IFN $\gamma$  three times weekly to prevent infections, which can serve as life-long protective treatment in these patients [77, 78]. The established safety and effectiveness of IFN $\gamma$  against these disorders and the ability of IFN $\gamma$  to

profoundly inhibit EBOV infection in our studies suggest that IFN $\gamma$  may serve as an EBOV antiviral therapy.

## Materials and Methods

### Ethics statement

The University of Iowa Institution Animal Care and Use Committee (IACUC) guidelines were followed for all animal experiments and breeding that took place at the University of Iowa. These guidelines are in strict adherence to the Public Health Service Policy on Humane Care and Use of Laboratory Animals and the University of Iowa OLAW Assurance Number is A3021-01. All animal studies performed at the University of Iowa in this study were approved by the University of Iowa IACUC under protocol #1203072.

Texas Biomedical Research Institute (TBRI) Institution Animal Care and Use Committee (IACUC) guidelines were following for all animal experiments that took place at TBRI. These guidelines are in strict adherence to the Public Health Service Policy on Humane Care and Use of Laboratory Animals and the TBRI OLAW Assurance Number is A3082-01. All animal studies performed at TBRI in this study were approved by the TBRI IACUC under protocol #1445MU1.

### Mice

BALB/c mice were obtained from the National Cancer Institute (Frederick, MD) and BALB/c IFN- $\alpha/\beta$  receptor-deficient (IFNAR<sup>-/-</sup>) mice were a kind gift from Dr. Joan Durbin, NYU Langone Medical Center. Wild-type C57BL/6 and IFN $\gamma$  receptor-deficient (IFN $\gamma$ R<sup>-/-</sup>) mice were a kind gift from Dr. John Hart, University of Iowa. Mice were bred at the University of Iowa.

Infectious EBOV mouse studies were performed in a biosafety level 4 laboratory (BSL4) at TBRI. For these studies, female BALB/c mice were obtained from Jackson Laboratory (Bar Harbor, ME) and housed under specific pathogen-free conditions.

### Production of virus

Recombinant wild-type EBOV expressing GFP for *in vitro* macrophage studies was generated as previously described [79]. Mouse adapted EBOV (MA-EBOV) was generated for *in vivo* mouse infections as previously described [80].

The production of recombinant, replication-competent vesicular stomatitis virus expressing eGFP and EBOV GP in place of the G glycoprotein (EBOV GP/rVSV) was performed as previously described [23, 25, 81]. The EBOV GP used in these studies was a GP lacking the mucin domain of GP1, which confers the same tropism as the full-length EBOV GP and produces higher titers [82–84]. EBOV GP/rVSV stocks were produced by infecting Vero cells at a low multiplicity of infection ( $\sim$ 0.001) and collecting supernatants 48 hours following infection. Virus-containing supernatants were filtered through a 0.45  $\mu$ m filter and stored at -80°C. EBOV GP/rVSV for mouse studies was concentrated by centrifugation at 7,000 x g at 4°C overnight. The virus pellet was resuspended and centrifuged through a 20% sucrose cushion by ultracentrifugation at 26,000 rpm for 2 hours at 4°C. The pellet was resuspended in PBS, aliquoted, and frozen at -80°C until use.

The generation of infectious VSV expressing eGFP utilized *in vivo* studies was previous described [85, 86]. VSV stocks were produced in Vero cells, concentrated and purified as described above.

## Primary cell isolation and cytokine stimulations

For isolation of murine peritoneal cells, mice were sacrificed and cells were harvested by lavage using 10 mL of ice-cold RPMI 1640 medium containing 10% FBS. The recovered peritoneal cells were washed in cold media and plated in the presence of 50 ng/mL of murine M-CSF (BioLegend, 576402). Non-adherent cells were removed 48 hours after isolation by washing twice with PBS. These adherent cells were previously characterized to express the macrophage surface markers, CD11b and F4/80 [87]. At 24 hours prior to infection, media was replaced with fresh media containing 50 ng/mL of murine M-CSF or GM-CSF with and without 20 ng/mL murine IFN $\gamma$  (Cell Sciences, CRI001B) and/or murine TNF $\alpha$  (BioLegend, 575202). Unless otherwise indicated in the figure legend, 20 ng/mL of IFN $\gamma$  was used for all studies.

The University of Iowa Institutional Review Board (IRB) approved all procedures for blood draws after obtaining informed consent from all individuals and all studies involving humans were performed under the approved University of Iowa IRB protocol #200607708 to Dr. Monick. Peripheral blood mononuclear cells (PBMCs) were isolated from human blood using Ficoll-Hypaque (Sigma-Aldrich), and monocyte-derived macrophages (MDMs) were isolated by adherence as previously described [88]. Isolated MDMs were plated in Dulbecco's modified Eagle medium (DMEM) (Gibco) media containing 10% fetal bovine serum (FBS) (Atlanta Biologicals), 10% Type AB human serum (Sigma), 1% penicillin/streptomycin (P/S) (Life Technologies) and 50 ng/mL of human M-CSF (R&D Systems). MDMs were differentiated for 6 days. After 6 days, media on the MDM cultures was replaced with media containing human M-CSF alone with or without the addition of 20 ng/mL of IFN $\gamma$  and/or TNF $\alpha$  (R&D Systems), unless otherwise indicated in the figure legend.

Human alveolar macrophages were isolated by bronchoalveolar lavage from healthy, consenting human volunteers as previously described [89]. Following isolation, the Wright-Giemsa-stained cytocentrifugation protocol was utilized to differentiate and count the total number of alveolar macrophages in the preparation. All cell preparations had between 90 and 100% alveolar macrophages [26, 27]. Alveolar macrophages were cultured in RPMI 1640 media containing 10% human serum, 10% FBS, 1% P/S and 50 ng/mL human M-CSF (R&D Systems) and stimulated with 20 ng/mL of human IFN $\gamma$  for 24 hours prior to infection.

## EBOV and EBOV GP/rVSV infections of macrophages

**EBOV.** BALB/c peritoneal macrophages were isolated by lavage as described above and plated in the presence of 50 ng/mL murine GM-CSF or M-CSF. For prophylactic treatment, cells were treated with 20 ng/mL of murine IFN $\gamma$  and/or murine TNF $\alpha$  for 24 hours prior to infection. Cells were refreshed with media without the addition of cytokines and transferred to a BSL4 facility at TBRI at 72 hours after cell isolation and challenged with replication-competent EBOV encoding GFP [79] at an MOI of 0.05. Cells were analyzed 24 hours following infection as described previously [25]. Briefly, the cells were fixed and stained with Hoescht 33342 dye and imaged with a Nikon Ti-Eclipse microscope using the high-content-analysis software package (Nikon, Tokyo, Japan). Images were processed and nuclei identified by Hoescht dye fluorescence. Total cells and cells expressing GFP were then counted using Cell Profiler software (Broad Institute, MIT, Boston, Massachusetts) using customized pipelines that are available from R. Davey upon request. Data are expressed as percent GFP positive cells.

**EBOV GP/rVSV.** Cytokine-containing media was removed from the macrophages and replaced with RPMI 1460 and 10% FCS. For the end point dilution assays, human and murine macrophage populations were infected with 10-fold serial dilutions of EBOV GP/rVSV (at least 4 replicates per dilution). Infection was scored 24 hours following infection for GFP

positivity using a fluorescent microscope. Virus titers were calculated as the 50% tissue culture infective dose (TCID<sub>50</sub>)/mL by the Reed-Meunch method [90].

For flow cytometric analysis, murine IFNAR<sup>-/-</sup> peritoneal macrophage infections were infected at an MOI of 0.1 based on titrating virus stocks on Vero cells. These infections were quantified by detecting GFP positivity using a FACS Calibur flow cytometer (BD Biosciences). Data were analyzed using FlowJo analysis software. Relative infection was quantified compared to M-CSF stimulated peritoneal macrophages that equaled 100%.

## Visualization of infected human alveolar macrophages

Alveolar macrophages were infected with EBOV GP/rVSV at an MOI of 5 at 48 hours following isolation and 18 hours after IFN $\gamma$  stimulation. Cells were fixed with 4% paraformaldehyde at 24 hours following EBOV GP/rVSV infection and covered with coverslips using Vectashield mounting medium with DAPI (H-1200; Vector Laboratories, Burlingame, CA). Images of alveolar macrophages were acquired using a Leica truepoint-scanning spectral system (TCS SPE) confocal microscope with Leica Application Suite (LAS AF) interface (Leica Microsystems, Wetzlar, Germany).

## Mouse cell RNA isolation and quantitative reverse transcriptase PCR

Murine macrophage cultures were isolated and maintained as described above. Cells were infected with EBOV GP/rVSV or MA-EBOV at an MOI of 0.1. When indicated, cells were incubated 15 minutes prior to and during infection with protein synthesis inhibitor cycloheximide (CHX) (Sigma) at a concentration of 10  $\mu$ g/mL [91]. Total RNA was isolated using the mirVana miRNA isolation kit (Ambion-Life Technologies) at 2, 6, 14 or 24 hours following infection. RNA was quantified by Nanodrop (Thermo Scientific). Total RNA (300 ng) was reverse-transcribed to cDNA using random primers and M-MLV reverse transcriptase (Invitrogen) using manufacturer's specifications. Quantitative reverse transcriptase polymerase chain reaction (qRT-PCR) was used to detect transcript levels. SYBR Green based quantitative PCR reactions (Applied Bioscience) were performed using specific primers to VSV (M or L), EBOV (NP or L) [92], proinflammatory cytokine/chemokines or ISGs and 2  $\mu$ L of cDNA from each reaction. Primer sequences are available upon request. Expression levels were defined as the ratio between threshold cycle (Ct) values and the housekeeping gene, HPRT. The determined ratios were converted to log<sub>2</sub> values. For the replication experiments, results are represented as fold change of log<sub>2</sub> values calculated based on the 2 or 6 hours M-CSF value.

## Human macrophage RNA extraction and microarray analysis

RNA preparation, quality analysis and microarray analysis were performed as previously described [93]. Microarrays assessed genome-wide macrophage mRNA expression using the GeneChip Human Exon 1.0 ST Arrays (Affymetrix). Microarray data were assessed by paired t-test and limma statistical analysis using R statistical software (<http://www.R-project.org>). Data were assessed for quality using a normalized unscaled standard error (NUSE) analysis. The method of statistical analysis was a paired t-test for each array. Limma analysis was performed to compare both macrophage arrays [94]. A 2-fold change in gene expression and *p* value of 0.01 was considered significant. Gene pathway analysis was conducted using GeneGo/Metacore version 6.19 (Thompson Reuters).

## Gene validation and analysis

Six of the top genes identified in the MDM and alveolar macrophage microarray analysis were validated by qRT-PCR as described above and previously described [93]. Primers specific for each of the ISGs were used to assess mRNA levels. Expression levels were defined as a ratio between threshold cycle values and housekeeping gene, HPRT. Primer sequences are available upon request.

## Interferon-stimulated gene inhibition studies

ISG-RFP lentiviral constructs were a kind gift from Dr. Charles Rice (Rockefeller University) and have been previously described [40]. HEK 293T cells stably expressing TIM-1 (H3 cells) [23], which are routinely tested for the absence of mycoplasma, were transfected with the ISG-RFP constructs at the indicated concentrations. Forty-eight hours following transfection, cells were infected with EBOV-GP/rVSV at MOI = 0.2. Infection was assessed using flow cytometry (BD FACSVerser) 24 hours following infection. Flow cytometry data were analyzed using FlowJo cytometry analysis software for percentage of RFP positive cells that were also GFP positive. Relative infection was determined based on infection of cells expressing RFP-control construct alone.

ISG inhibition of infectious EBOV virus was performed using Neon (Invitrogen) electroporated HeLa cells (Ambion, Austin, TX). Forty-eight hours following transfection, cells were infected with EBOV-GFP at MOI of 0.5. After 24 hours, infection was quantified as described previously [25]. Briefly, images were analyzed using Cell Profiler to quantify RFP and GFP positive cells. Data were analyzed with FCS Express analysis software and cells were gated based on the no infection control.

## IRF1 siRNA knockdown of EBOV GP/rVSV infection by exosome delivery

**Isolation of exosomes.** The day before exosome collection the culture medium of HEK 293T cells was replaced with DMEM supplemented with pre-spun FBS. To avoid contamination of FBS derived exosomes, FBS were spun at 100,000  $\times g$  for 2 hours. The culture supernatants from the HEK 293T cells were collected and the exosomes were isolated from the supernatant by differential centrifugation as described previously [95, 96]. In brief, the cell supernatants were cleared of intact cells and cell debris by centrifugation at 1000  $\times g$  for 10 minutes and 10000  $\times g$  for 30 minutes at 4°C, and then supernatant was subjected to filtration through a 0.22  $\mu m$  Amicon filter. The supernatants were concentrated in a 100 kDa MWCO Centricon Plus-15 (Millipore) to 1–2 mL. The concentrated supernatants were spun at 100,000  $\times g$  for 70 minutes in TLA 100.3 rotor (Beckman Coulter) to pellet exosomes. The collected exosomes were washed twice in PBS. The recovery of exosomes was estimated by measuring the protein concentration using Bradford assay.

**Exosomes labeling and confocal imaging.** Exosomes were loaded with 1X CellMask Deep Red Plasma Membrane stain for 10 minutes at 37°C. Exosomes were then washed with PBS and centrifuged at 100,000  $\times g$  for 70 minutes in TLA 100.3 rotor (Beckman Coulter) to pellet exosomes and resuspended in culture medium.

For imaging, peritoneal macrophages (300,000 cells) were allowed to attach in eight-well chamber slides. Ten micrograms of exosomes loaded with CellMask were applied to peritoneal macrophages and imaged 24 hour following treatment. Exosome uptake was visualized by on a Leica TCS SP3 confocal microscope (Leica Microsystems Inc., Buffalo Grove IL). Cells were

fixed in 2% paraformaldehyde and mounted with Vectashield with DAPI (Vector Laboratories Inc., Burlingame, CA) before imaging.

**Loading of DsiRNA into exosomes.** Dicer-substrate RNAs (DsiRNA) (IDT), 27mer duplex RNAs that have increased potency in RNA interference compared to traditional siRNAs [97], were loaded into exosomes by electroporation as described [98]. Briefly, exosome pellets were resuspended in electroporation buffer for siRNA loading. The electroporation mixture was prepared by mixing exosomes and DsiRNA in 1:1 (wt/wt) in electroporation buffer. The final concentration of exosomes in the mixture was 250 ng/ $\mu$ L. The mixture was electroporated in a 400  $\mu$ L volume using 0.4-mm cuvettes at 400 mV and 125  $\mu$ F capacitance with pulse time of 10–15 ms. Exosomes were aliquoted and frozen at -20°C until use.

**Exosome IRF1 knockdown and EBOV GP/rVSV infections.** BALB/c IFNAR<sup>-/-</sup> peritoneal macrophages were isolated as described above and cultured 250,000 cells in a 96-well format in the presence of 50ng/mL M-CSF for 48 hours prior to addition of DsiRNA loaded exosomes. IRF1 or scrambled (Scr) siRNA loaded exosomes (2.5  $\mu$ g) were added to macrophages in fresh media with fresh M-CSF with or without 20ng/mL IFN $\gamma$ . Macrophages and exosomes were spinoculated by centrifugation at 700 x g at 4°C for 1 hour and then incubated at 37°C for 24 hours. Twenty-four hours later, all media, exosomes and cytokines were removed and macrophages were infected with fresh media containing EBOV GP/rVSV at an MOI of 0.1. Twenty-four hours following infection, cells were lysed as described above for RNA extraction. RNA isolation, cDNA synthesis and quantification of IRF1/VSV-L expression by qPCR were performed as described above. Expression levels were defined as the ratio between threshold cycle (Ct) values for IRF1 or VSV-L and the housekeeping gene, mouse HPRT, and is displayed as the log<sub>2</sub> value of this ratio.

## Mouse infections

**EBOV GP/rVSV and VSV infections.** Five- to eight-week-old male BALB/c IFNAR<sup>-/-</sup> mice were administered recombinant murine (rm)-IFN $\gamma$  (1, 3.3 or 10  $\mu$ g/mouse as noted in figure legends of specific studies) (Cell Sciences, CRI001B) or PBS by intraperitoneal (i.p.) or intramuscular (i.m.) injection. Twenty-four hours after IFN $\gamma$  injection, mice were infected with 10<sup>3</sup> infectious units of EBOV GP/rVSV or 10<sup>2</sup> infectious units of VSV virus by i.p. injection. In parallel experiments, other mice were administered IFN $\gamma$  2, 6, 12 or 48 hours following EBOV GP/rVSV infection by i.p. injection. In the VSV studies, post challenge administration of IFN $\gamma$  was given only at 2 hours following infection. Mice were weighed and scored for sickness daily. Clinical sickness scoring was as follows: 0, no apparent illness; 1, slightly ruffled fur; 2, ruffled fur, active; 3, ruffled fur, inactive; 4, ruffled fur, inactive, hunched posture; 5, moribund or dead. Results represent scores from at least 10 mice per group. All mouse infection studies were concluded at 10 or 12 days following infection due to surviving mice regaining any lost weight and having no signs of clinical illness.

**MA-EBOV infections.** Five-week-old female BALB/c mice were administered rm-IFN $\gamma$  (Cell Sciences, CRI001B) at the indicated concentration or PBS by i.p. injection 24 hours prior to, at the time, 6 or 24 hours following virus challenge. All of the mice were injected i.p. with 1000 plaque forming units (PFU) of mouse-adapted EBOV [99]. Mice were observed daily for weight loss and clinical scores. All surviving animals were sacrificed at day 12 or 14.

## Serum/organ viral titers

**EBOV GP/rVSV infections.** Organs were harvested 2 days following infection from at least 4 mice from each treatment group. Mice were anesthetized with isofluorene to perform retro-orbital bleeds for serum. Mice were euthanized and perfused with 10 mL of PBS through

the heart prior to harvesting organs. The total peritoneal cell population was isolated and lysed for qRT-PCR to detect viral RNA as described above. Organs were homogenized in PBS and titers were determined by end-point dilution as described above on mycoplasma-free Vero cells.

**MA-EBOV infections.** Four days following infection, three animals per group were sacrificed, sera was isolated from blood samples and stored at  $-80^{\circ}\text{C}$  until use. Virus loads were quantified by culturing 10-fold serial dilutions of serum in PBS on mycoplasma free Vero-E6 cells seeded in 6 well plates. After a one hour incubation, the supernatant was replaced with DMEM containing methylcellulose with 2% FBS and cells were incubated at  $37^{\circ}\text{C}$  for 10 days. Cells were fixed in 10% formalin overnight and stained with crystal violet. Plaques were manually counted.

## Statistical analysis

No statistical method was used to predetermine sample size. Tissue culture experiments were performed at least in triplicate with at least three replicates per experiment. *In vivo* survival experiments were performed at least in duplicate with at least 7 mice per treatment group. MA-EBOV or EBOV GP/rVSV titer studies were performed with at least three mice for each treatment group. When possible for both *in vitro* and *in vivo* studies, the investigators or veterinary staff were blinded to group allocation during the experiment and when assessing the outcome. Mice or samples were randomly assigned to various treatment groups. All data points and animals were reported in results and statistical analyses.

Statistical analyses were performed using GraphPad Prism software (GraphPad Software, Inc.). Results are shown as means  $\pm$  standard error of the means (s.e.m.). Two-tailed, unpaired Student's *t*-tests were used to compare experimental treatment group to no IFN $\gamma$  control for the majority of the studies reported here. To assess variance in these studies, F tests to compare variance were performed in parallel to determine that variance was similar between groups. For protein translation inhibition studies, a one-way analysis of variance (ANOVA) was performed to compare the no IFN $\gamma$  control to the different treatments followed by a Tukey post hoc multiple comparison analysis to determine statistical significance. For nonparametric data, Mann-Whitney U-test was used. Log-rank (Mantel-Cox) tests were used to analyze differences in survival. *P* values less than 0.05 were considered significant.

## Supporting Information

**S1 Fig. IFN $\gamma$  increases expression of proinflammatory cytokines IL-6 and TNF $\alpha$  and chemokines, CXCL10.** M-CSF treated BALB/c peritoneal macrophages were untreated or stimulated with IFN $\gamma$  24 hours prior to infection. A subset of macrophages was infected with EBOV (MOI = 0.1) under BSL-4 conditions. Total RNA was harvested and cytokine/chemokine RNA expression quantified by qRT-PCR. Results represent means  $\pm$  s.e.m. Data were analyzed by Student's *t*-test compared to M-CSF control, \**p* < 0.05, \*\**p* < 0.01; ns, not significantly different.

(TIF)

**S2 Fig. IFN $\gamma$ , not TNF $\alpha$ , inhibits EBOV GP/rVSV infection of BALB/c and C57BL/6 murine macrophages.** (A) M-CSF-treated BALB/c peritoneal macrophages were stimulated with IFN $\gamma$ , TNF $\alpha$  or the combination for 24 hours prior to EBOV GP/rVSV (MOI = 0.1) infection. Infection was quantified 24 hours following addition of virus by GFP positivity of the culture. (B) IFN $\gamma$ , but not TNF $\alpha$ , inhibits EBOV GP/rVSV infection of M-CSF-treated C57BL/6 peritoneal macrophages. TCID<sub>50</sub> values were determined by 10-fold serial dilutions of virus on

to the macrophage cultures and titers assessed at 24 hours of infection by end-point dilution. Results represent means  $\pm$  s.e.m. Data were analyzed by Student's t-test compared to M-CSF-treated cells, \*\* $p < 0.01$ , \*\*\* $p < 0.001$ , \* $p < 0.05$ .

(TIF)

**S3 Fig. IFN $\gamma$  inhibition of EBOV GP/rVSV infection does not require the IFN $\alpha/\beta$  receptor, but does require the IFN $\gamma$  receptor.** (A) IFN $\gamma$  inhibition of EBOV GP/rVSV infection is independent of the interferon  $\alpha/\beta$  receptor (IFNAR) in BALB/c and C57BL/6 IFNAR<sup>-/-</sup> peritoneal macrophages. M-CSF-treated cells were stimulated with IFN $\gamma$ . Twenty-four hours later, cells were infected with EBOV GP/rVSV (MOI = 0.1) and assessed for GFP expression 24 hours following infection by flow cytometry. (B) Increasing concentrations of IFN $\gamma$  block EBOV GP/rVSV (MOI = 0.1) in C57BL/6 IFNAR<sup>-/-</sup> peritoneal macrophages in a dose-dependent manner. GFP expression was assessed at 24 hours by flow cytometry. (C) IFN $\gamma$  receptor is required for IFN $\gamma$  inhibition of EBOV GP/rVSV in mouse peritoneal macrophages. Peritoneal macrophages from C57BL/6 IFN $\gamma$ R<sup>-/-</sup> mice were infected with 10-fold serial dilutions of EBOV GP/rVSV and virus titers were determined by end point dilution. Results represent means  $\pm$  s.e.m. Data were analyzed by Student's or one-sample t-test, \* $p < 0.05$ , \*\* $p < 0.01$ , \*\*\* $p < 0.001$ . ns, not significantly different.

(TIF)

**S4 Fig. IFN $\gamma$  inhibits EBOV GP/rVSV RNA production to the same extent as a protein synthesis inhibitor, CHX.** Total RNA was isolated at 6 hours following EBOV GP/rVSV infection for qRT-PCR for VSV matrix (M) and polymerase (L) RNA. Results are represented as log<sub>2</sub> values. Significance determined by ANOVA with a Tukey post-test. \*\*\* $p < 0.01$  (compared to M-CSF alone). ns, not significantly different.

(TIF)

**S5 Fig. Identification of IFN $\gamma$ -responsive genes in human alveolar macrophages.** (A) Differential gene expression profile of IFN $\gamma$ -responsive genes in human alveolar macrophages. Genes were clustered into annotated ontology groups and listed in the corresponding GO groups table with their respective GO terms. Significance was determined by paired t-test analysis with cutoff values of at least two-fold change and  $p < 0.01$ . NUSE analysis of the array demonstrated that the means were centered at a value of 1 and minimum and maximum values between 0.95 and 1.05. ISGs that were assessed further in this study are bolded in the GO table. (B) mRNA validation of human alveolar macrophage profiling results for several of the most statistically significant IFN $\gamma$  stimulated genes. RNA obtained for the microarray analysis was assessed for mRNA levels of the selected genes by qRT-PCR. Results are represented as the log<sub>2</sub> values. Significance was determined by t-test analysis, \* $p < 0.05$ , \*\* $p < 0.01$ .

(TIF)

**S6 Fig. Identification of statistically significant genes identified in both gene arrays of IFN $\gamma$ -stimulated human MDMs and alveolar macrophages.** (A) A merged differential gene expression profile of IFN $\gamma$ -responsive genes of our hMDM and human alveolar macrophage gene arrays. ISGs that were assessed further in this study are bolded. Significance was determined by limma analysis with cutoff values of at least two-fold change and  $p < 0.01$ . MDM, monocyte derived macrophages. AM, alveolar macrophages. (B) Identification of IFN $\gamma$  differentially regulated gene pathways in macrophages. Representative bar graph displays the relative number of IFN $\gamma$  responsive genes from both macrophage microarrays. Stripped bars, number of genes identified to correlate with each pathway that are represented in both the MDM and alveolar macrophage gene array datasets. Solid blue, genes unique to the MDM gene array

results. Solid orange bars, genes unique to the alveolar macrophage gene array results. (TIF)

**S7 Fig. HEK 293T exosomes are engulfed by murine peritoneal macrophages.** Exosomes were isolated from HEK 293T cells and loaded with CellMask Deep Red Plasma Membrane stain. Exosomes (10 $\mu$ g) were washed and applied to BALB/c IFNAR<sup>-/-</sup> peritoneal macrophages for 24 hours. Cells were washed, fixed and exosome uptake was visualized by confocal microscopy. DAPI stained nuclei (blue), actin (green) and exosomes (red). (TIF)

**S8 Fig. IFN $\gamma$  decreases morbidity and mortality associated with *in vivo* EBOV GP/rVSV and VSV infections.** (A) IFN $\gamma$  protects against weight loss by EBOV GP/rVSV infection at both 3.3 and 10  $\mu$ g of murine IFN $\gamma$ . Murine IFN $\gamma$  (1, 3.3 or 10  $\mu$ g) or PBS was administered 24 hours prior to infection with 10<sup>3</sup> infectious units (iu) of EBOV GP/rVSV. Data represent 3 mice per group from 2 independent experiments. Death of mice at a particular day is indicated by a cross and value indicating the number of mice that succumb to infection. (B) IFN $\gamma$  enhances survival of EBOV GP/rVSV infected mice and more modestly enhances survival following wild-type VSV infection. 3.3  $\mu$ g IFN $\gamma$  or PBS was administered by i.p. injection to BALB/c IFNAR<sup>-/-</sup> mice 24 hours prior to or 2 hours following 10<sup>3</sup> iu of EBOV GP/rVSV or 10<sup>2</sup> iu VSV infection (n $\geq$ 8/treatment). Protection studies with 3.3  $\mu$ g of IFN $\gamma$  were also performed at 6 hours following EBOV GP/rVSV challenge. Significance was determined by Mantel-Cox Test; compared to EBOV GP/rVSV PBS mice, \*\*  $p < 0.01$ , \*\*\*  $p < 0.001$ , compared to VSV PBS mice, #  $p < 0.05$ , ###  $p < 0.001$ , compared EBOV GP/rVSV IFN $\gamma$  treated groups to VSV IFN $\gamma$  treated groups,  $\partial p < 0.05$ . (C) Treatment of mice with 10  $\mu$ g IFN $\gamma$  24 hours prior to or 2, 6, 12 or 48 hours following EBOV GP/rVSV infection prevents weight loss during the first 3 days of EBOV GP/rVSV *in vivo* infection. (D) IFN $\gamma$  (10  $\mu$ g) treatment protects against weight loss at early days following infection. IFN $\gamma$  was given 24 hours prior or 2, 6, 12 or 48 hours following EBOV GP/rVSV. For C and D, results represent means  $\pm$  s.e.m. For B-D, treatment groups consist of at least 8 mice per group. Significance was determined by Student's t-test compared to PBS control, \*\*\*  $p < 0.001$ . (TIF)

**S9 Fig. IFN $\gamma$  decreases morbidity and mortality associated with *in vivo* MA-EBOV infections.** (A) Mice treated with 10  $\mu$ g of IFN $\gamma$  are protected from mortality associated with MA-EBOV infection. Doses of IFN $\gamma$  or PBS were administered by i.p. injection to BALB/c mice 24 h prior to MA-EBOV infection. Significance was determined by Mantel-Cox Test, \*\*\*  $p < 0.001$ . (B) Weight loss of MA-EBOV infected mice following IFN $\gamma$  treatment. Results represent means  $\pm$  s.e.m. (C) Clinical sickness scores following MA-EBOV infection and IFN $\gamma$  treatment. Findings in panels A-C represent 7 mice per group from one experiment. (D) IFN $\gamma$  treatment inhibits MA-EBOV viremia. Serum was collected 4 days following infection and viral loads quantified with 10-fold serial dilutions of serum on Vero-E6 cells to determine PFU/mL. Data represent 2 or 3 mice per group. Significance was determined by Student's t-test compared to PBS control, \*  $p < 0.05$ . (TIF)

**S1 Table. IFN $\gamma$  stimulated genes significantly altered in human MDMs treated with 20 ng/ml of IFN $\gamma$  as assessed by gene array analysis.** ISGs that were assessed further in this study are bolded. (XLSX)

**S2 Table. IFN $\gamma$  stimulated genes significantly altered in human alveolar macrophages treated with 20 ng/ml of IFN $\gamma$  as assessed by gene array analysis.** ISGs that were assessed further in this study are bolded.

(XLSX)

## Acknowledgments

We thank Dr. Stanley Perlman and Rachel Brouillette for providing helpful comments on the manuscript.

## Author Contributions

Conceived and designed the experiments: BAR RAD MMM WM. Performed the experiments: BAR LSP MA YS CMH MMM WM BKS KR PS. Analyzed the data: BAR LSP MA YS TB CMH RAD MMM WM KR BS PS RAD. Contributed reagents/materials/analysis tools: TB PS. Wrote the paper: BAR RAD MMM WM.

## References

1. Leroy EM, Gonzalez JP, Baize S. Ebola and Marburg haemorrhagic fever viruses: major scientific advances, but a relatively minor public health threat for Africa. *Clinical microbiology and infection: the official publication of the European Society of Clinical Microbiology and Infectious Diseases*. 2011; 17(7):964–76. PMID: [21722250](#).
2. Gire SK, Goba A, Andersen KG, Sealfon RS, Park DJ, Kanneh L, et al. Genomic surveillance elucidates Ebola virus origin and transmission during the 2014 outbreak. *Science (New York, NY)*. 2014; 345(6202):1369–72. doi: [10.1126/science.1259657](#) PMID: [25214632](#).
3. Geisbert TW, Young HA, Jahrling PB, Davis KJ, Larsen T, Kagan E, et al. Pathogenesis of Ebola hemorrhagic fever in primate models: evidence that hemorrhage is not a direct effect of virus-induced cytolysis of endothelial cells. *The American journal of pathology*. 2003; 163(6):2371–82. Epub 2003/11/25. PMID: [14633609](#); PubMed Central PMCID: PMC1892396.
4. Bray M, Geisbert TW. Ebola virus: the role of macrophages and dendritic cells in the pathogenesis of Ebola hemorrhagic fever. *The international journal of biochemistry & cell biology*. 2005; 37(8):1560–6. Epub 2005/05/18. doi: [10.1016/j.biocel.2005.02.018](#) PMID: [15896665](#).
5. Gupta M, Mahanty S, Ahmed R, Rollin PE. Monocyte-derived human macrophages and peripheral blood mononuclear cells infected with ebola virus secrete MIP-1alpha and TNF-alpha and inhibit poly-IC-induced IFN-alpha in vitro. *Virology*. 2001; 284(1):20–5. PMID: [11352664](#).
6. Hensley LE, Young HA, Jahrling PB, Geisbert TW. Proinflammatory response during Ebola virus infection of primate models: possible involvement of the tumor necrosis factor receptor superfamily. *Immunology letters*. 2002; 80(3):169–79. PMID: [11803049](#).
7. Geisbert TW, Young HA, Jahrling PB, Davis KJ, Kagan E, Hensley LE. Mechanisms underlying coagulation abnormalities in ebola hemorrhagic fever: overexpression of tissue factor in primate monocytes/macrophages is a key event. *The Journal of infectious diseases*. 2003; 188(11):1618–29. doi: [10.1086/379724](#) PMID: [14639531](#).
8. Bray M, Mahanty S. Ebola hemorrhagic fever and septic shock. *The Journal of infectious diseases*. 2003; 188(11):1613–7. Epub 2003/11/26. doi: [10.1086/379727](#) PMID: [14639530](#).
9. Stroher U, West E, Bugany H, Klenk HD, Schnittler HJ, Feldmann H. Infection and activation of monocytes by Marburg and Ebola viruses. *Journal of virology*. 2001; 75(22):11025–33. Epub 2001/10/17. PMID: [11602743](#); PubMed Central PMCID: PMC114683.
10. Sanchez A, Lukwiya M, Bausch D, Mahanty S, Sanchez AJ, Wagoner KD, et al. Analysis of human peripheral blood samples from fatal and nonfatal cases of Ebola (Sudan) hemorrhagic fever: cellular responses, virus load, and nitric oxide levels. *Journal of virology*. 2004; 78(19):10370–7. PMID: [15367603](#); PubMed Central PMCID: PMC516433.
11. Jahrling PB, Geisbert TW, Geisbert JB, Swarengen JR, Bray M, Jaax NK, et al. Evaluation of immune globulin and recombinant interferon-alpha2b for treatment of experimental Ebola virus infections. *The Journal of infectious diseases*. 1999; 179 Suppl 1:S224–34. Epub 1999/02/13. PMID: [9988188](#).
12. Smith LM, Hensley LE, Geisbert TW, Johnson J, Stossel A, Honko A, et al. Interferon-beta therapy prolongs survival in rhesus macaque models of Ebola and Marburg hemorrhagic fever. *The Journal of*

- infectious diseases. 2013; 208(2):310–8. doi: [10.1093/infdis/jis921](https://doi.org/10.1093/infdis/jis921) PMID: [23255566](https://pubmed.ncbi.nlm.nih.gov/23255566/); PubMed Central PMCID: [PMC3685222](https://pubmed.ncbi.nlm.nih.gov/PMC3685222/).
13. Qiu X, Wong G, Fernando L, Audet J, Bello A, Strong J, et al. mAbs and Ad-vectored IFN-alpha therapy rescue Ebola-infected nonhuman primates when administered after the detection of viremia and symptoms. *Science translational medicine*. 2013; 5(207):207ra143. Epub 2013/10/18. doi: [10.1126/scitranslmed.3006605](https://doi.org/10.1126/scitranslmed.3006605) PMID: [24132638](https://pubmed.ncbi.nlm.nih.gov/24132638/).
  14. Murray PJ, Allen JE, Biswas SK, Fisher EA, Gilroy DW, Goerdts S, et al. Macrophage activation and polarization: nomenclature and experimental guidelines. *Immunity*. 2014; 41(1):14–20. doi: [10.1016/j.immuni.2014.06.008](https://doi.org/10.1016/j.immuni.2014.06.008) PMID: [25035950](https://pubmed.ncbi.nlm.nih.gov/25035950/); PubMed Central PMCID: [PMC4123412](https://pubmed.ncbi.nlm.nih.gov/PMC4123412/).
  15. Martinez FO, Gordon S. The M1 and M2 paradigm of macrophage activation: time for reassessment. *F1000prime reports*. 2014; 6:13. doi: [10.12703/P6-13](https://doi.org/10.12703/P6-13) PMID: [24669294](https://pubmed.ncbi.nlm.nih.gov/24669294/); PubMed Central PMCID: [PMC3944738](https://pubmed.ncbi.nlm.nih.gov/PMC3944738/).
  16. Sica A, Mantovani A. Macrophage plasticity and polarization: in vivo veritas. *The Journal of clinical investigation*. 2012; 122(3):787–95. doi: [10.1172/JCI59643](https://doi.org/10.1172/JCI59643) PMID: [22378047](https://pubmed.ncbi.nlm.nih.gov/22378047/); PubMed Central PMCID: [PMC3287223](https://pubmed.ncbi.nlm.nih.gov/PMC3287223/).
  17. Liu SY, Sanchez DJ, Aliyari R, Lu S, Cheng G. Systematic identification of type I and type II interferon-induced antiviral factors. *Proceedings of the National Academy of Sciences of the United States of America*. 2012; 109(11):4239–44. doi: [10.1073/pnas.1114981109](https://doi.org/10.1073/pnas.1114981109) PMID: [22371602](https://pubmed.ncbi.nlm.nih.gov/22371602/); PubMed Central PMCID: [PMC3306696](https://pubmed.ncbi.nlm.nih.gov/PMC3306696/).
  18. Morrow AN, Schmeisser H, Tsuno T, Zoon KC. A novel role for IFN-stimulated gene factor 3II in IFN-gamma signaling and induction of antiviral activity in human cells. *Journal of immunology (Baltimore, Md: 1950)*. 2011; 186(3):1685–93. doi: [10.4049/jimmunol.1001359](https://doi.org/10.4049/jimmunol.1001359) PMID: [21178011](https://pubmed.ncbi.nlm.nih.gov/21178011/); PubMed Central PMCID: [PMC3417313](https://pubmed.ncbi.nlm.nih.gov/PMC3417313/).
  19. Schroder K, Hertzog PJ, Ravasi T, Hume DA. Interferon-gamma: an overview of signals, mechanisms and functions. *Journal of leukocyte biology*. 2004; 75(2):163–89. PMID: [14525967](https://pubmed.ncbi.nlm.nih.gov/14525967/).
  20. Towner JS, Paragas J, Dover JE, Gupta M, Goldsmith CS, Huggins JW, et al. Generation of eGFP expressing recombinant Zaire ebolavirus for analysis of early pathogenesis events and high-throughput antiviral drug screening. *Virology*. 2005; 332(1):20–7. Epub 2005/01/22. doi: [10.1016/j.virol.2004.10.048](https://doi.org/10.1016/j.virol.2004.10.048) PMID: [15661137](https://pubmed.ncbi.nlm.nih.gov/15661137/).
  21. Carette JE, Raaben M, Wong AC, Herbert AS, Obernosterer G, Mulherkar N, et al. Ebola virus entry requires the cholesterol transporter Niemann-Pick C1. *Nature*. 2011; 477(7364):340–3. Epub 2011/08/26. doi: [10.1038/nature10348](https://doi.org/10.1038/nature10348) PMID: [21866103](https://pubmed.ncbi.nlm.nih.gov/21866103/); PubMed Central PMCID: [PMC3175325](https://pubmed.ncbi.nlm.nih.gov/PMC3175325/).
  22. Miller EH, Obernosterer G, Raaben M, Herbert AS, Deffieu MS, Krishnan A, et al. Ebola virus entry requires the host-programmed recognition of an intracellular receptor. *The EMBO journal*. 2012; 31(8):1947–60. Epub 2012/03/08. doi: [10.1038/emboj.2012.53](https://doi.org/10.1038/emboj.2012.53) PMID: [22395071](https://pubmed.ncbi.nlm.nih.gov/22395071/); PubMed Central PMCID: [PMC3343336](https://pubmed.ncbi.nlm.nih.gov/PMC3343336/).
  23. Kondratowicz AS, Lennemann NJ, Sinn PL, Davey RA, Hunt CL, Moller-Tank S, et al. T-cell immunoglobulin and mucin domain 1 (TIM-1) is a receptor for Zaire Ebolavirus and Lake Victoria Marburgvirus. *Proceedings of the National Academy of Sciences of the United States of America*. 2011; 108(20):8426–31. doi: [10.1073/pnas.1019030108](https://doi.org/10.1073/pnas.1019030108) PMID: [21536871](https://pubmed.ncbi.nlm.nih.gov/21536871/); PubMed Central PMCID: [PMC3100998](https://pubmed.ncbi.nlm.nih.gov/PMC3100998/).
  24. Irie T, Carnero E, Garcia-Sastre A, Harty RN. In Vivo Replication and Pathogenesis of Vesicular Stomatitis Virus Recombinant M40 Containing Ebola Virus L-Domain Sequences. *Infectious diseases*. 2012; 5:59–64. Epub 2013/06/25. doi: [10.4137/idrt.s10652](https://doi.org/10.4137/idrt.s10652) PMID: [23794798](https://pubmed.ncbi.nlm.nih.gov/23794798/); PubMed Central PMCID: [PMC3686127](https://pubmed.ncbi.nlm.nih.gov/PMC3686127/).
  25. Moller-Tank S, Kondratowicz AS, Davey RA, Rennert PD, Maury W. Role of the phosphatidylserine receptor TIM-1 in enveloped-virus entry. *Journal of virology*. 2013; 87(15):8327–41. doi: [10.1128/JVI.01025-13](https://doi.org/10.1128/JVI.01025-13) PMID: [23698310](https://pubmed.ncbi.nlm.nih.gov/23698310/); PubMed Central PMCID: [PMC3719829](https://pubmed.ncbi.nlm.nih.gov/PMC3719829/).
  26. Monick MM, Carter AB, Gudmundsson G, Geist LJ, Hunninghake GW. Changes in PKC isoforms in human alveolar macrophages compared with blood monocytes. *The American journal of physiology*. 1998; 275(2 Pt 1):L389–97. Epub 1998/08/12. PMID: [9700101](https://pubmed.ncbi.nlm.nih.gov/9700101/).
  27. Monick MM, Carter AB, Hunninghake GW. Human alveolar macrophages are markedly deficient in REF-1 and AP-1 DNA binding activity. *The Journal of biological chemistry*. 1999; 274(25):18075–80. Epub 1999/06/11. PMID: [10364260](https://pubmed.ncbi.nlm.nih.gov/10364260/).
  28. Plataniias LC. Mechanisms of type-I- and type-II-interferon-mediated signalling. *Nature reviews Immunology*. 2005; 5(5):375–86. PMID: [15864272](https://pubmed.ncbi.nlm.nih.gov/15864272/).
  29. Taniguchi T, Takaoka A. A weak signal for strong responses: interferon-alpha/beta revisited. *Nature reviews Molecular cell biology*. 2001; 2(5):378–86. PMID: [11331912](https://pubmed.ncbi.nlm.nih.gov/11331912/).

30. Ling PD, Warren MK, Vogel SN. Antagonistic effect of interferon-beta on the interferon-gamma-induced expression of Ia antigen in murine macrophages. *Journal of immunology (Baltimore, Md: 1950)*. 1985; 135(3):1857–63. PMID: [3926890](#).
31. Yoshida R, Murray HW, Nathan CF. Agonist and antagonist effects of interferon alpha and beta on activation of human macrophages. Two classes of interferon gamma receptors and blockade of the high-affinity sites by interferon alpha or beta. *The Journal of experimental medicine*. 1988; 167(3):1171–85. PMID: [2965208](#); PubMed Central PMCID: PMC2188875.
32. Martinez O, Johnson JC, Honko A, Yen B, Shabman RS, Hensley LE, et al. Ebola virus exploits a monocyte differentiation program to promote its entry. *Journal of virology*. 2013; 87(7):3801–14. Epub 2013/01/25. doi: [10.1128/jvi.02695-12](#) PMID: [23345511](#); PubMed Central PMCID: PMC3624207.
33. Knipe DM, Howley PM. *Fields virology*. 6th ed. Philadelphia, PA: Wolters Kluwer/Lippincott Williams & Wilkins Health; 2013. 2 volumes p.
34. Marcus PI, Engelhardt DL, Hunt JM, Sekellick MJ. Interferon action: inhibition of vesicular stomatitis virus RNA synthesis induced by virion-bound polymerase. *Science (New York, NY)*. 1971; 174(4009):593–8. PMID: [4329841](#).
35. Schoggins JW. Interferon-stimulated genes: roles in viral pathogenesis. *Current opinion in virology*. 2014; 6:40–6. doi: [10.1016/j.coviro.2014.03.006](#) PMID: [24713352](#); PubMed Central PMCID: PMC4077717.
36. Gough DJ, Messina NL, Hii L, Gould JA, Sabapathy K, Robertson AP, et al. Functional crosstalk between type I and II interferon through the regulated expression of STAT1. *PLoS biology*. 2010; 8(4): e1000361. Epub 2010/05/04. doi: [10.1371/journal.pbio.1000361](#) PMID: [20436908](#); PubMed Central PMCID: PMCPmc2860501.
37. Galindo-Moreno J, Iurlaro R, El Mjiyad N, Diez-Perez J, Gabaldon T, Munoz-Pinedo C. Apolipoprotein L2 contains a BH3-like domain but it does not behave as a BH3-only protein. *Cell death & disease*. 2014; 5:e1275. doi: [10.1038/cddis.2014.237](#) PMID: [24901046](#).
38. Luo C, Chen M, Madden A, Xu H. Expression of complement components and regulators by different subtypes of bone marrow-derived macrophages. *Inflammation*. 2012; 35(4):1448–61. doi: [10.1007/s10753-012-9458-1](#) PMID: [22450524](#).
39. Schoggins JW, Rice CM. Interferon-stimulated genes and their antiviral effector functions. *Current opinion in virology*. 2011; 1(6):519–25. Epub 2012/02/14. doi: [10.1016/j.coviro.2011.10.008](#) PMID: [22328912](#); PubMed Central PMCID: PMC3274382.
40. Schoggins JW, Wilson SJ, Panis M, Murphy MY, Jones CT, Bieniasz P, et al. A diverse range of gene products are effectors of the type I interferon antiviral response. *Nature*. 2011; 472(7344):481–5. Epub 2011/04/12. doi: [10.1038/nature09907](#) PMID: [21478870](#); PubMed Central PMCID: PMC3409588.
41. Audette M, Larouche L, Lussier I, Fugere N. Stimulation of the ICAM-1 gene transcription by the peroxovanadium compound [bpV(Pic)] involves STAT-1 but not NF-kappa B activation in 293 cells. *European journal of biochemistry / FEBS*. 2001; 268(6):1828–36. Epub 2001/03/15. PMID: [11248703](#).
42. Yokosawa N, Yokota S, Kubota T, Fujii N. C-terminal region of STAT-1alpha is not necessary for its ubiquitination and degradation caused by mumps virus V protein. *Journal of virology*. 2002; 76(24):12683–90. Epub 2002/11/20. PMID: [12438594](#); PubMed Central PMCID: PMCPmc136684.
43. Wen Z, Zhong Z, Darnell JE Jr., Maximal activation of transcription by Stat1 and Stat3 requires both tyrosine and serine phosphorylation. *Cell*. 1995; 82(2):241–50. Epub 1995/07/28. PMID: [7543024](#).
44. Yee JK, Friedmann T, Burns JC. Generation of high-titer pseudotyped retroviral vectors with very broad host range. *Methods in cell biology*. 1994; 43 Pt A:99–112. Epub 1994/01/01. PMID: [7823872](#).
45. Hastie E, Cataldi M, Marriott I, Grdzlishvili VZ. Understanding and altering cell tropism of vesicular stomatitis virus. *Virus research*. 2013; 176(1–2):16–32. Epub 2013/06/26. doi: [10.1016/j.virusres.2013.06.003](#) PMID: [23796410](#); PubMed Central PMCID: PMCPmc3865924.
46. Younes HM, Amsden BG. Interferon- $\gamma$  therapy: Evaluation of routes of administration and delivery systems. *Journal of pharmaceutical sciences*. 2002; 91(1):2–17. PMID: [11782893](#)
47. Janardhana V, Tachedjian M, Cramer G, Cowled C, Wang LF, Baker ML. Cloning, expression and antiviral activity of IFN $\gamma$  from the Australian fruit bat, *Pteropus alecto*. *Developmental and comparative immunology*. 2012; 36(3):610–8. Epub 2011/11/19. doi: [10.1016/j.dci.2011.11.001](#) PMID: [22093696](#).
48. Consales CA, Mendonca RZ, Gallina NM, Pereira CA. Cytopathic effect induced by rabies virus in McCoy cells. *Journal of virological methods*. 1990; 27(3):277–85. Epub 1990/03/01. PMID: [1691201](#).
49. Barkhouse DA, Garcia SA, Bongiorno EK, Lebrun A, Faber M, Hooper DC. Expression of interferon gamma by a recombinant rabies virus strongly attenuates the pathogenicity of the virus via induction of type I interferon. *Journal of virology*. 2015; 89(1):312–22. Epub 2014/10/17. doi: [10.1128/jvi.01572-14](#) PMID: [25320312](#); PubMed Central PMCID: PMCPmc4301114.

50. Cheon H, Holvey-Bates EG, Schoggins JW, Forster S, Hertzog P, Imanaka N, et al. IFN $\beta$ -dependent increases in STAT1, STAT2, and IRF9 mediate resistance to viruses and DNA damage. *The EMBO journal*. 2013; 32(20):2751–63. Epub 2013/09/26. doi: [10.1038/emboj.2013.203](https://doi.org/10.1038/emboj.2013.203) PMID: [24065129](https://pubmed.ncbi.nlm.nih.gov/24065129/); PubMed Central PMCID: PMCPmc3801437.
51. Schoggins JW, MacDuff DA, Imanaka N, Gainey MD, Shrestha B, Eitson JL, et al. Pan-viral specificity of IFN-induced genes reveals new roles for cGAS in innate immunity. *Nature*. 2014; 505(7485):691–5. doi: [10.1038/nature12862](https://doi.org/10.1038/nature12862) PMID: [24284630](https://pubmed.ncbi.nlm.nih.gov/24284630/); PubMed Central PMCID: PMC4077721.
52. Maloney NS, Thackray LB, Goel G, Hwang S, Duan E, Vachharajani P, et al. Essential cell-autonomous role for interferon (IFN) regulatory factor 1 in IFN- $\gamma$ -mediated inhibition of norovirus replication in macrophages. *Journal of virology*. 2012; 86(23):12655–64. Epub 2012/09/14. doi: [10.1128/jvi.01564-12](https://doi.org/10.1128/jvi.01564-12) PMID: [22973039](https://pubmed.ncbi.nlm.nih.gov/22973039/); PubMed Central PMCID: PMCPmc3497668.
53. Man SM, Karki R, Malireddi RK, Neale G, Vogel P, Yamamoto M, et al. The transcription factor IRF1 and guanylate-binding proteins target activation of the AIM2 inflammasome by Francisella infection. *Nature immunology*. 2015; 16(5):467–75. Epub 2015/03/17. doi: [10.1038/ni.3118](https://doi.org/10.1038/ni.3118) PMID: [25774715](https://pubmed.ncbi.nlm.nih.gov/25774715/); PubMed Central PMCID: PMCPmc4406811.
54. Jouvenet N, Neil SJ, Zhadina M, Zang T, Kratovac Z, Lee Y, et al. Broad-spectrum inhibition of retroviral and filoviral particle release by tetherin. *Journal of virology*. 2009; 83(4):1837–44. Epub 2008/11/28. doi: [10.1128/jvi.02211-08](https://doi.org/10.1128/jvi.02211-08) PMID: [19036818](https://pubmed.ncbi.nlm.nih.gov/19036818/); PubMed Central PMCID: PMCPmc2643743.
55. Okumura A, Pitha PM, Harty RN. ISG15 inhibits Ebola VP40 VLP budding in an L-domain-dependent manner by blocking Nedd4 ligase activity. *Proceedings of the National Academy of Sciences of the United States of America*. 2008; 105(10):3974–9. Epub 2008/02/29. doi: [10.1073/pnas.0710629105](https://doi.org/10.1073/pnas.0710629105) PMID: [18305167](https://pubmed.ncbi.nlm.nih.gov/18305167/); PubMed Central PMCID: PMCPmc2268823.
56. Malakhova OA, Zhang DE. ISG15 inhibits Nedd4 ubiquitin E3 activity and enhances the innate antiviral response. *The Journal of biological chemistry*. 2008; 283(14):8783–7. Epub 2008/02/22. doi: [10.1074/jbc.C800030200](https://doi.org/10.1074/jbc.C800030200) PMID: [18287095](https://pubmed.ncbi.nlm.nih.gov/18287095/); PubMed Central PMCID: PMCPmc2276364.
57. Spiropoulou CF, Ranjan P, Pearce MB, Sealy TK, Albarino CG, Gangappa S, et al. RIG-I activation inhibits ebolavirus replication. *Virology*. 2009; 392(1):11–5. Epub 2009/07/25. doi: [10.1016/j.virol.2009.06.032](https://doi.org/10.1016/j.virol.2009.06.032) PMID: [19628240](https://pubmed.ncbi.nlm.nih.gov/19628240/).
58. Reid SP, Leung LW, Hartman AL, Martinez O, Shaw ML, Carbonnelle C, et al. Ebola virus VP24 binds karyopherin alpha1 and blocks STAT1 nuclear accumulation. *Journal of virology*. 2006; 80(11):5156–67. Epub 2006/05/16. PMID: [16698996](https://pubmed.ncbi.nlm.nih.gov/16698996/); PubMed Central PMCID: PMCPmc1472181.
59. Toth K, Lee SR, Ying B, Spencer JF, Tollefson AE, Sagartz JE, et al. STAT2 Knockout Syrian Hamsters Support Enhanced Replication and Pathogenicity of Human Adenovirus, Revealing an Important Role of Type I Interferon Response in Viral Control. *PLoS pathogens*. 2015; 11(8):e1005084. Epub 2015/08/21. doi: [10.1371/journal.ppat.1005084](https://doi.org/10.1371/journal.ppat.1005084) PMID: [26291525](https://pubmed.ncbi.nlm.nih.gov/26291525/); PubMed Central PMCID: PMCPmc4546297.
60. Huang IC, Bailey CC, Weyer JL, Radoshitzky SR, Becker MM, Chiang JJ, et al. Distinct patterns of IFITM-mediated restriction of filoviruses, SARS coronavirus, and influenza A virus. *PLoS pathogens*. 2011; 7(1):e1001258. doi: [10.1371/journal.ppat.1001258](https://doi.org/10.1371/journal.ppat.1001258) PMID: [21253575](https://pubmed.ncbi.nlm.nih.gov/21253575/); PubMed Central PMCID: PMC3017121.
61. Williams BR, Kerr IM. Inhibition of protein synthesis by 2'-5' linked adenine oligonucleotides in intact cells. *Nature*. 1978; 276(5683):88–90. PMID: [740027](https://pubmed.ncbi.nlm.nih.gov/740027/).
62. Taylor MW, Feng GS. Relationship between interferon- $\gamma$ , indoleamine 2,3-dioxygenase, and tryptophan catabolism. *FASEB journal: official publication of the Federation of American Societies for Experimental Biology*. 1991; 5(11):2516–22. PMID: [1907934](https://pubmed.ncbi.nlm.nih.gov/1907934/).
63. Bach EA, Aguet M, Schreiber RD. The IFN  $\gamma$  receptor: a paradigm for cytokine receptor signaling. *Annual review of immunology*. 1997; 15:563–91. PMID: [9143700](https://pubmed.ncbi.nlm.nih.gov/9143700/).
64. Young HA. Regulation of interferon- $\gamma$  gene expression. *Journal of interferon & cytokine research: the official journal of the International Society for Interferon and Cytokine Research*. 1996; 16(8):563–8. PMID: [8877725](https://pubmed.ncbi.nlm.nih.gov/8877725/).
65. Bosio CM, Aman MJ, Grogan C, Hogan R, Ruthel G, Negley D, et al. Ebola and Marburg viruses replicate in monocyte-derived dendritic cells without inducing the production of cytokines and full maturation. *The Journal of infectious diseases*. 2003; 188(11):1630–8. Epub 2003/11/26. doi: [10.1086/379199](https://doi.org/10.1086/379199) PMID: [14639532](https://pubmed.ncbi.nlm.nih.gov/14639532/).
66. Mahanty S, Hutchinson K, Agarwal S, McRae M, Rollin PE, Pulendran B. Cutting edge: impairment of dendritic cells and adaptive immunity by Ebola and Lassa viruses. *Journal of immunology (Baltimore, Md: 1950)*. 2003; 170(6):2797–801. Epub 2003/03/11. PMID: [12626527](https://pubmed.ncbi.nlm.nih.gov/12626527/).
67. Audet J, Kobinger GP. Immune evasion in ebolavirus infections. *Viral immunology*. 2015; 28(1):10–8. Epub 2014/11/15. doi: [10.1089/vim.2014.0066](https://doi.org/10.1089/vim.2014.0066) PMID: [25396298](https://pubmed.ncbi.nlm.nih.gov/25396298/).

68. Baize S, Leroy EM, Georges-Courbot MC, Capron M, Lansoud-Soukate J, Debre P, et al. Defective humoral responses and extensive intravascular apoptosis are associated with fatal outcome in Ebola virus-infected patients. *Nature medicine*. 1999; 5(4):423–6. PMID: [10202932](#).
69. Baize S, Leroy EM, Georges AJ, Georges-Courbot MC, Capron M, Bedjabaga I, et al. Inflammatory responses in Ebola virus-infected patients. *Clinical and experimental immunology*. 2002; 128(1):163–8. PMID: [11982604](#); PubMed Central PMCID: PMC1906357.
70. Bente D, Gren J, Strong JE, Feldmann H. Disease modeling for Ebola and Marburg viruses. *Disease models & mechanisms*. 2009; 2(1–2):12–7. doi: [10.1242/dmm.000471](#) PMID: [19132113](#); PubMed Central PMCID: PMC2615158.
71. Bradfute SB, Warfield KL, Bray M. Mouse models for filovirus infections. *Viruses*. 2012; 4(9):1477–508. Epub 2012/11/22. doi: [10.3390/v4091477](#) PMID: [23170168](#); PubMed Central PMCID: PMC3499815.
72. Nakayama E, Saijo M. Animal models for Ebola and Marburg virus infections. *Frontiers in microbiology*. 2013; 4:267. doi: [10.3389/fmicb.2013.00267](#) PMID: [24046765](#); PubMed Central PMCID: PMC3763195.
73. Cooksley WG. Treatment of hepatitis B with interferon and combination therapy. *Clinics in liver disease*. 2004; 8(2):353–70. PMID: [15481344](#).
74. Shepherd J, Waugh N, Hewitson P. Combination therapy (interferon alfa and ribavirin) in the treatment of chronic hepatitis C: a rapid and systematic review. *Health technology assessment*. 2000; 4(33):1–67. PMID: [11134916](#).
75. Todd PA, Goa KL. Interferon gamma-1b. A review of its pharmacology and therapeutic potential in chronic granulomatous disease. *Drugs*. 1992; 43(1):111–22. PMID: [1372855](#).
76. Key LL Jr., Ries WL, Rodriguiz RM, Hatcher HC. Recombinant human interferon gamma therapy for osteopetrosis. *The Journal of pediatrics*. 1992; 121(1):119–24. PMID: [1320672](#).
77. Nuno H, Ishibashi F, Mizukami T, Hidaka F. Clinical evaluation of interferon-gamma treatment to chronic granulomatous disease patients with splice site mutations. *Japanese journal of infectious diseases*. 2004; 57(5):S25–6. PMID: [15507763](#).
78. Marciano BE, Wesley R, De Carlo ES, Anderson VL, Barnhart LA, Darnell D, et al. Long-term interferon-gamma therapy for patients with chronic granulomatous disease. *Clinical infectious diseases: an official publication of the Infectious Diseases Society of America*. 2004; 39(5):692–9. PMID: [15356785](#).
79. Ebihara H, Theriault S, Neumann G, Alimonti JB, Geisbert JB, Hensley LE, et al. In vitro and in vivo characterization of recombinant Ebola viruses expressing enhanced green fluorescent protein. *The Journal of infectious diseases*. 2007; 196 Suppl 2:S313–22. doi: [10.1086/520590](#) PMID: [17940966](#).
80. Bray M, Davis K, Geisbert T, Schmaljohn C, Huggins J. A mouse model for evaluation of prophylaxis and therapy of Ebola hemorrhagic fever. *The Journal of infectious diseases*. 1998; 178(3):651–61. PMID: [9728532](#).
81. Gao Y, Whitaker-Dowling P, Watkins SC, Griffin JA, Bergman I. Rapid adaptation of a recombinant vesicular stomatitis virus to a targeted cell line. *Journal of virology*. 2006; 80(17):8603–12. doi: [10.1128/JVI.00142-06](#) PMID: [16912309](#); PubMed Central PMCID: PMC1563842.
82. Yang ZY, Duckers HJ, Sullivan NJ, Sanchez A, Nabel EG, Nabel GJ. Identification of the Ebola virus glycoprotein as the main viral determinant of vascular cell cytotoxicity and injury. *Nature medicine*. 2000; 6(8):886–9. PMID: [10932225](#).
83. Jeffers SA, Sanders DA, Sanchez A. Covalent modifications of the ebola virus glycoprotein. *Journal of virology*. 2002; 76(24):12463–72. PMID: [12438572](#); PubMed Central PMCID: PMC136726.
84. Sinn PL, Hickey MA, Staber PD, Dylla DE, Jeffers SA, Davidson BL, et al. Lentivirus vectors pseudotyped with filoviral envelope glycoproteins transduce airway epithelia from the apical surface independently of folate receptor alpha. *Journal of virology*. 2003; 77(10):5902–10. PMID: [12719583](#); PubMed Central PMCID: PMC154009.
85. Whelan SP, Barr JN, Wertz GW. Identification of a minimal size requirement for termination of vesicular stomatitis virus mRNA: implications for the mechanism of transcription. *Journal of virology*. 2000; 74(18):8268–76. Epub 2000/08/23. PMID: [10954524](#); PubMed Central PMCID: PMC16335.
86. Cherry S, Doukas T, Armknecht S, Whelan S, Wang H, Sarnow P, et al. Genome-wide RNAi screen reveals a specific sensitivity of IRES-containing RNA viruses to host translation inhibition. *Genes & development*. 2005; 19(4):445–52. Epub 2005/02/17. doi: [10.1101/gad.1267905](#) PMID: [15713840](#); PubMed Central PMCID: PMC1548945.
87. Lennemann NJ, Rhein BA, Ndungo E, Chandran K, Qiu X, Maury W. Comprehensive functional analysis of N-linked glycans on Ebola virus GP1. *mBio*. 2014; 5(1):e00862–13. Epub 2014/01/30. doi: [10.1128/mBio.00862-13](#) PMID: [24473128](#); PubMed Central PMCID: PMC3950510.

88. Maury W. Monocyte maturation controls expression of equine infectious anemia virus. *Journal of virology*. 1994; 68(10):6270–9. PMID: [8083967](#); PubMed Central PMCID: PMC237047.
89. Gross TJ, Powers LS, Boudreau RL, Brink B, Reisetter A, Goel K, et al. A microRNA processing defect in smokers' macrophages is linked to SUMOylation of the endonuclease DICER. *The Journal of biological chemistry*. 2014; 289(18):12823–34. doi: [10.1074/jbc.M114.565473](#) PMID: [24668803](#); PubMed Central PMCID: PMC4007470.
90. Reed LJ, Muench H. A simple method of estimating fifty percent endpoints. *American Journal of Epidemiology*. 1938; 27(3):493–7.
91. Whelan SP, Wertz GW. Transcription and replication initiate at separate sites on the vesicular stomatitis virus genome. *Proceedings of the National Academy of Sciences of the United States of America*. 2002; 99(14):9178–83. doi: [10.1073/pnas.152155599](#) PMID: [12089339](#); PubMed Central PMCID: PMC123114.
92. Shabman RS, Hoenen T, Groseth A, Jabado O, Binning JM, Amarasinghe GK, et al. An upstream open reading frame modulates ebola virus polymerase translation and virus replication. *PLoS pathogens*. 2013; 9(1):e1003147. doi: [10.1371/journal.ppat.1003147](#) PMID: [23382680](#); PubMed Central PMCID: PMC3561295.
93. Gerke AK, Pezzulo AA, Tang F, Cavanaugh JE, Bair TB, Phillips E, et al. Effects of vitamin D supplementation on alveolar macrophage gene expression: preliminary results of a randomized, controlled trial. *Multidisciplinary respiratory medicine*. 2014; 9(1):18. doi: [10.1186/2049-6958-9-18](#) PMID: [24669961](#); PubMed Central PMCID: PMC3986866.
94. Smyth G. Limma: linear models for microarray data. In: 'Bioinformatics and Computational Biology Solutions using R and Bioconductor'. R. Gentleman VC, Dudoit S., Irizarry R., Huber W. editor. New York: Springer; 2005. 397–420 p.
95. Raposo G, Nijman HW, Stoorvogel W, Liejendekker R, Harding CV, Melief CJ, et al. B lymphocytes secrete antigen-presenting vesicles. *The Journal of experimental medicine*. 1996; 183(3):1161–72. Epub 1996/03/01. PMID: [8642258](#); PubMed Central PMCID: PMC3561295.
96. Thery C, Amigorena S, Raposo G, Clayton A. Isolation and characterization of exosomes from cell culture supernatants and biological fluids. *Current protocols in cell biology / editorial board, Juan S Bonifacino [et al]*. 2006; Chapter 3:Unit 3 22. doi: [10.1002/0471143030.cb0322s30](#) PMID: [18228490](#).
97. Kim DH, Behlke MA, Rose SD, Chang MS, Choi S, Rossi JJ. Synthetic dsRNA Dicer substrates enhance RNAi potency and efficacy. *Nature biotechnology*. 2005; 23(2):222–6. Epub 2004/12/28. doi: [10.1038/nbt1051](#) PMID: [15619617](#).
98. El-Andaloussi S, Lee Y, Lakhali-Littleton S, Li J, Seow Y, Gardiner C, et al. Exosome-mediated delivery of siRNA in vitro and in vivo. *Nature protocols*. 2012; 7(12):2112–26. Epub 2012/11/17. PMID: [23154783](#).
99. Bray M, Davis K, Geisbert T, Schmaljohn C, Huggins J. A mouse model for evaluation of prophylaxis and therapy of Ebola hemorrhagic fever. *The Journal of infectious diseases*. 1999; 179 Suppl 1:S248–58. PMID: [9988191](#).